We are IntechOpen,
the world's leading publisher of
Open Access books
Built by scientists, for scientists

4,800

Open access books available

122,000

International authors and editors

135M

Downloads

Our authors are among the

154

Countries delivered to

TOP 1%

most cited scientists

12.2%

Contributors from top 500 universities

BOOK CITATION INDEX INDEXED — CLARIVATE ANALYTICS

WEB OF SCIENCE™

Selection of our books indexed in the Book Citation Index
in Web of Science™ Core Collection (BKCI)

Interested in publishing with us?
Contact book.department@intechopen.com

Numbers displayed above are based on latest data collected.
For more information visit www.intechopen.com

Effluent Cleaning, Greener Catalysts and Bioecomaterials from Agricultural Wastes

A.M. Martínez Serrano, M. Ramos, M. Yates, M.A. Martin-Luengo, F. Plou, J.L. Lacomba, G. Reilly, C. Vervaet, P. Muñoz, G. Garcia, J.L. Tarterra, B. Fite, A. Urtzainki, M.C. Vidal, E. Sáez Rojo, L. Vega Argomaniz, A. Civantos and V. Zurdo

Additional information is available at the end of the chapter

http://dx.doi.org/10.5772/60018

1. Introduction

The transformation of subproducts and residues is of utmost importance, especially when it closes an industrial cycle, where solutions for environmental problems such as contamination leads towards a sustainable development, converting residues into value added products. Materials prepared from agricultural residues may be considered as Renewable Raw Materials [1,2]. Using these materials as a source for useful materials avoids the expense of employing other materials that are often non-renewable. This philosophy is denoted as "cradle to grave", since the residues of a company are used by the same or others [3].

Agriculture is one of the pillars of society, especially given the increasing world population. Countries which have large agricultural resources, such as Spain, also produce vast amounts of residues and wastes, that can be an environmental hazard, difficult to store, easily generating leakages and greenhouse gases such as ammonia, methane and carbon, nitrogen and sulphur oxides when burnt, therefore negatively impacting on the environment. However, these agriwastes can also be considered as a source of low cost renewable raw materials (RRM) that with the proper treatment can have applications in a wide range of processes, *i.e.* energy production, materials (fertilizers, animal feed, biodegradable plastics, resins, textiles, fibres, paper, *etc.*) and chemicals (platform molecules, solvents, additives), inside the Biorefinery concept, with the added bonus of not competing with food resources [4].

The work presented here uses agricultural wastes to prepare materials for effluent cleaning with rice and beer production wastes, etherification of glycerol from biodiesel production,

enzyme immobilisation and use in biodiesel preparation and Bioecomaterials for tissue engineering and controlled desorption of bioactive substances.

2. Effluent cleaning with materials derived from rice and beer production wastes

Industrial effluents often have high flows with variable concentrations of toxic substances, where adsorption is an ideal process for their decontamination due to its good economic turnover and the possibility of recovering the contaminants by desorption. The process of adsorption is based on the diffusion of sorbates to the adsorbent surface, followed by the inclusion inside the pore structure where they are stored. Here the textural properties of the adsorbents (surface area and porosity) are of the utmost importance [5].

Distilleries Muñoz Galvez (DMG) is a leading Spanish Company that manufactures and exports Essential Oils and Aromatic Raw Materials (Fine Chemicals) as well as Fragrances and Flavours worldwide [6]. The challenge faced by the research group (CDTI project) [7] was to clean DMG wastewaters that contained terpenes as the main residue, as expected given their origin, thus reducing water consumption, economic expenditure and possible environmental hazards. Aiming to decrease the economic costs, and increase the project´s environmental approach, agriresidues from beer and rice production were used to prepare materials capable of wastewater decontamination that were compared to commercial adsorbents. Previous knowledge of the researchers was applied and optimised to the wastewater composition and treatments [8,9]. The results indicated better adsorption and therefore cleaning capacities in the residue derived materials than in the commercial ones. The chemical oxygen demands after wastewater treatment were low enough for the treated water to be discharged in accordance with the legal requirements.

The agriresidues chosen for this study were beer bagasse and rice husk. Beer bagasse, from Mahou San Miguel (Spain) [10] (designated as BBM), is a residue from beer production that has *ca*. 75-80% water. Previous work by the authors has demonstrated that materials prepared from beer bagasse are basic due to their high P, Si, Ca and Mg content. Furthermore, due to their origin these materials are competitive in price; in fact BBM is at present used as a fertiliser [11].

Rice husk (RH) from DACSA (Spain) [12] is an agriresidue from rice production, of difficult storage and transport due to its high volume to weight ratio. On calcining this residue, a material with more than 97% silica is produced, that has also low amounts of calcium and potassium [13-15].

The agriresidues utilized as raw materials in this study were used as received, in the case of rice husk, or after a drying step at 150°C in the case of the BBM, to inhibit further fermentation due to its high water content. The RH and the dried BBM were analysed by TG-DTA in air to determine their thermal stabilities and design the material preparation. Details of experimental set up can be found in [14]. Figure 1 shows these data.
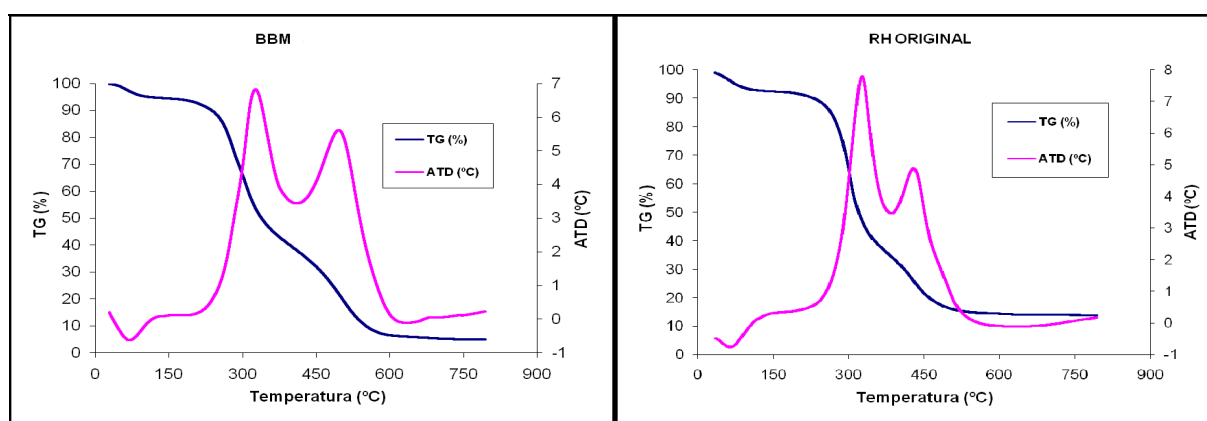
Figure 1. TG-DTA analyses of RH and BBM agriresidues in air.

From these results the agriresidues loose up to 90 (BBM) and 87 (RH) percent weight, when calcined up to 800°C, where the weight losses were an endotherm due to water loss up to 200 °C and two exotherms at 340 °C and 520 °C (BBM) or 340 °C and 470 °C (RH) due to decomposition/transformation of the organic matter to volatile organic substances and carbonization [14].

After studying the reproducibility of the materials the temperature chosen to prepare the adsorbents through thermal treatment of the agriresidues was 350 °C for 2, 4 or 6 h. These materials were designated as BBM2, BBM4, BBM6, RH2, RH4 and RH6. The composition analyses of these agriresidue derived materials are included in Table 1. From these results it was clear that under these conditions the materials derived from BBM were mainly carbonaceous whilst those derived from RH have siliceous structure and the content of the elements that form volatile species (CO_2, H_2O, NO_X, oxychlorides, *etc.*) decreased on increasing the time of thermal treatment, while the percentage of the other elements increased.

	BBM2	BBM4	BBM6	RH2	RH4	RH6
C	43.1	43.2	40.1	7.0	1.8	1.0
H	1.6	1.6	1.6	0.7	0.4	0.3
N	11.3	10.2	2.5	0.5	0.2	0.1
Al	0.3	0.2	0.0	0.0	0.0	0.0
Na	0.1	0.1	0.1	0.1	0.1	0.2
Mg	1.2	1.6	1.7	0.4	0.4	0.4
Si	2.1	5.6	7.9	42.1	52.0	55.6
P	1.5	3.5	5.6	0.4	0.5	0.5
S	0.2	0.2	0.2	0.2	0.2	0.2
Cl	0.0	0.0	0.1	0.0	0.0	0.1
K	0.2	0.4	0.6	2.3	3.4	3.6
Ca	0.9	1.6	2.5	0.9	1.1	1.1
Fe	0.1	0.1	0.2	0.1	0.1	0.2
Zn	0.0	0.0	0.1	0.0	0.0	0.1

Table 1. Percent composition of agriresidue derived materials (Traces: Ti, Cr, Ni, Ga, Br, Rb, Mn, Sr, Cu).

Textural analyses of the agriresidue derived materials were carried out by mercury intrusion porosimetry (MIP) and the data obtained are included in Figure 2 and Table 2. Description by the authors of the experimental analyses for MIP can be found in reference 16.

In this technique, the pores below 300 nm correspond to those inside the particles, while those at higher values are due to interparticle voids. As can be seen in all the materials prepared, the curves coincide for values below 1000 nm. As expected, in general, there was an increase in the total pore volume on increasing the calcination time, due to decomposition of volatile compounds, producing extra porosity, in agreement with TG-DTA analyses.
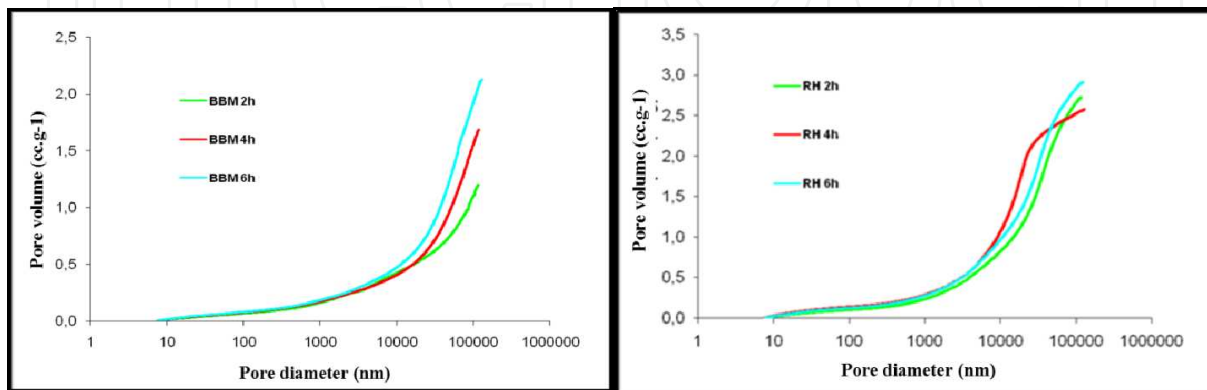
Figure 2. MIP textural data of agriresidue derived materials.

	S_{Hg} (m²/g)	Vp (cm³/g)	Porosity (%)	dp (nm)
BBM2	16	0.18	66.7	25.4
BBM4	18	0.18	69.2	44.7
BBM6	20	0.19	75.9	67.1
RH2	27	0.24	81.0	36.1
RH4	33	0.25	82.3	48.3
RH6	38	0.26	84.7	67.9
Fluesorb B	52	0.22	44.6	10.2

Table 2. Textural characteristics of agriresidue derived materials and an Activated Carbon by MIP. *(S$_{Hg}$= Specific surace area, Vp = Pore Volume, dp = medium pore size.*

From this data it can be observed that the porosity, surface area and medium pore size increase with time of calcination and the surface areas were lower but the pore sizes higher for the residue derived materials compared to the commercial activated carbon.

The analysis of DMG wastewater was carried out by GCMS (Figure 3), the experimental details for this technique can be found in reference 17. From these analyses the presence of *ca.* 16 different substances was found (Figure 3) and for the quantification of the cleaning studies, the main substances (9.5 min (pinene), 13.6 min (limonene), 18.1 min (hexadecyl acetate), 19.5min ($C_{19}H_{40}$), 22 min ($C_{20}H_{42}$), 26.2 min ($C_{21}H_{44}$) and 27.5 min ($C_{22}H_{46}$) were chosen.
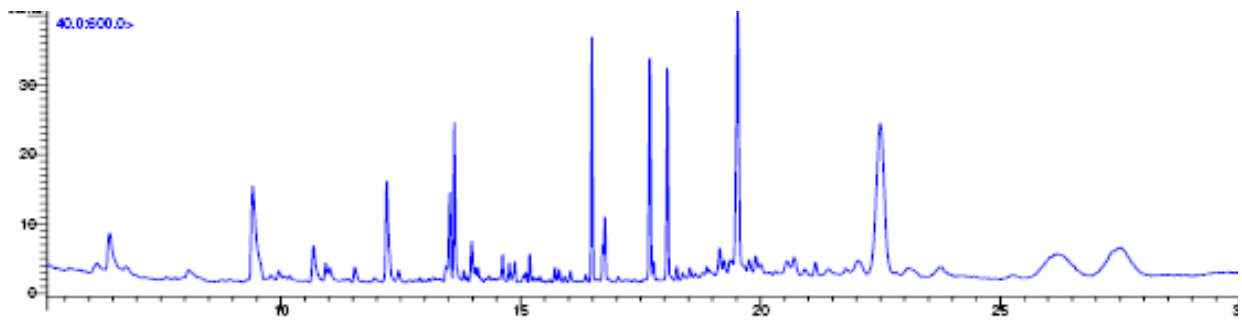
Figure 3. GCMS analysis of DMG wastewater.

The DMG wastewater treatments were carried out by using 0.5 g of carbon (commercial or Ecomaterial), and 30 mL of the DMG wastewater (to ensure reproducibility of the measurements), these slurries were magnetically stirred and 2 mL aliquots of the original and treated wastewaters were extracted at increasing times with the same volume of di-isopropylether, dried over sodium sulphate and analysed by GCMS (Figures 4 and 5).
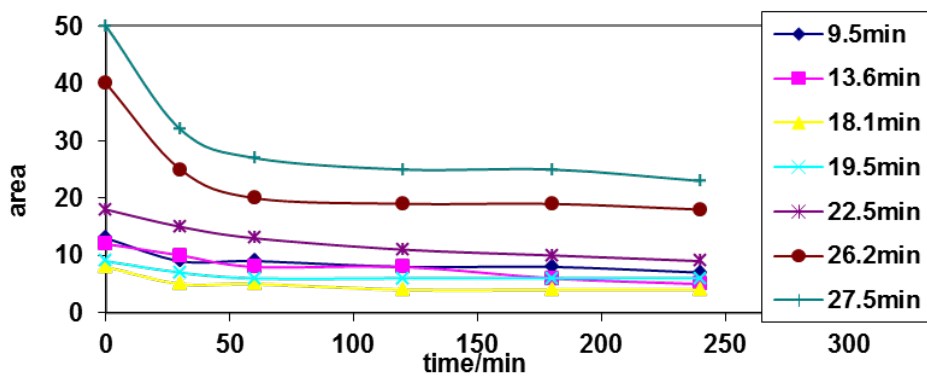

Figure 4. DMG Wastewater cleaning on BBM2.
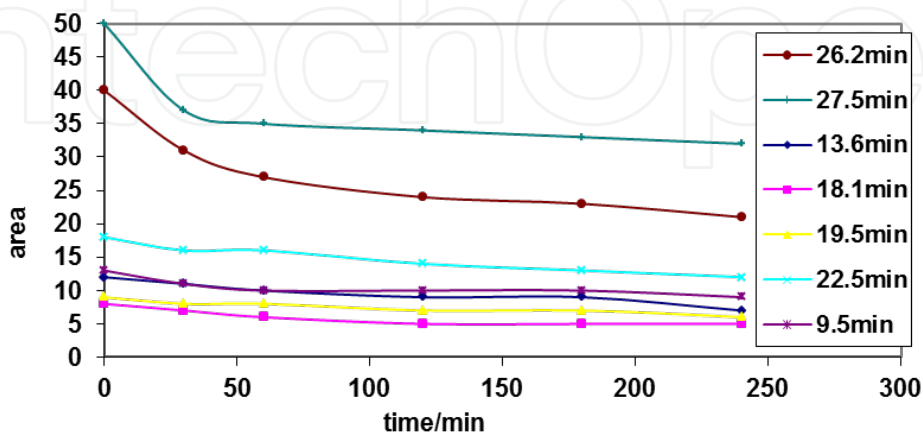
Figure 5. DMG Wastewater cleaning on Fluesorb B.

These results indicated that the carbon prepared from beer residues had better adsorption capacities for cleaning the DMG wastewater than the commercial one, especially with regards to the high molecular weight substances. This can be related to the different textures, since the commercial carbon has smaller pores that can not easily accommodate the high molecular weight substances. The chemical oxygen demand (COD) of the original and treated wastewaters was studied according to the Spanish UNE 77004, equivalent to ISO 6060:1989:

$$DQO: \frac{800 \times C \times (V_1 - V_2)}{V_0}$$

where C: concentration of Fe(II) sulphate and ammoniumin mol/L, V_0: volume in mL before dilution, V_1: volume in mL of Fe(II) sulphate and ammonium solution for blank analysis, V_2: is the volume in mL of Fe(II) sulphate and ammonium solution for assay, 8000 is molar mass in mg/L of ½ O_2. The COD results are in mg O_2/L. The value of the method has been checked with a 0.425 g of potassium hydrogenphtalate ($KC_8H_5O_4$), dried at 105°C, diluted in 1000 mL distilled water with a COD standard value of 500 mg O_2/L (+/- 20). Variabilities in COD analyses were less than 2 % [18]. The results obtained for the COD reduction of the wastewater, with the different materials are included in Table 3 (Percent reduction of COD after room temperature wastewater treatment with adsorbents until constant COD (usually *ca*. 60 minutes).

	COD % Reduction
Comercial (Fluesorb B)	4
BBM2	5
BBM4	10
BBM6	18
RH2	17
RH4	67
RH6	73

Table 3. Percent COD reduction of DMG wastewater with adsorbents.

The high effectiveness of the residue derived materials compared with the commercial carbon should be noted. The material with greater cleaning ability was RH6 (73% reduction), which allowed a water with COD of 960 mg O_2 /L. Comparing the textural data with COD determinations, it can be said that there was a direct correlation between the pore diameter of the solids and their COD reduction capacity. Thus, wastewater treatment with residue derived materials has been shown to be an economical and environmentally sound process that should be further developed [19].

3. Etherification of glycerol from biodiesel production with company´s own residues

The need for renewable energies in general and biodiesel in particular, indicates that optimising the production process is of vital importance. Biodiesel production generates *ca.* 10% of glycerol as a subproduct which has led to a fall in the glycerol prices, making the search for other industrial applications a neccesity. Amongst all possible processes to increase the value of glycerol, etherification is one of the most promising, since glycerol ethers can be used as such or with slight modification as fuel additives [20]. Other important uses are found in cosmetics, food additives, monomers for polimerisation processes *etc.* [21].

This research was undertaken with the aim to use Acesur-Tarancon´s own subproducts to prepare catalysts to transform the company´s glycerol (from their biodiesel plant) to diglicerol ethers. The catalysts prepared in this way are in fact Ecomaterials and their origin makes them competitive with commercial ones. Production of ethers with more than three glycerol molecules competes with diethers and thus control of the selectitivy is important, especially keeping in mind that the diglycerol ethers (Figure 6) are produced at short reaction times, which gives the process an added value [20, 22].
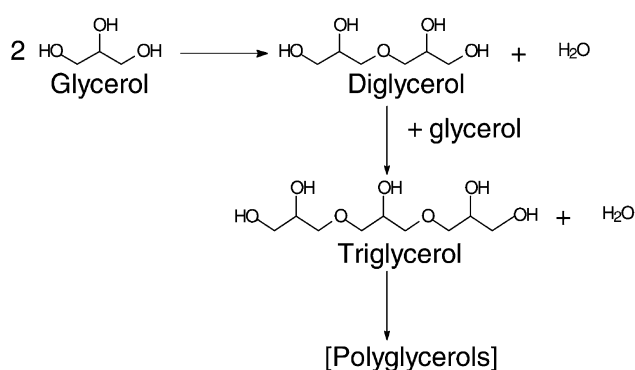
Figure 6. Glycerol pathway to di- and triglycerols in reference 23.

Etherification of glycerol with acid catalysts was found to be difficult to control. However, the catalytic transformation of glycerol into ethers, carried out with basic catalysts allows more controllable results. Furthermore, the use of heterogeneous catalysts *i.e.* alkaline and alkaline earth oxides, present in the residue derived materials form Acesur, compared to homogeneous bases is gaining interest since they are easily separated from the reactants and products for reuse with the corresponding economic benefits [24]. A bibliographic search showed Barrault ´s work describing caesium oxide catalysts that achieved medium conversions with selectivities to di- and triglycerols, depending mainly on the reaction time [25]. Also Ruppert describes a reaction carried out on alkaline-earth oxides at 220 °C for 20 h giving rise to higher glycerol conversions on the more basic catalysts: 5 % (MgO), 58 % (CaO), 80 % (SrO) and 80 % (BaO) [26].

The oligoglycerols are gaining more and more interest as products used in cosmetics, food-additives or lubricants [27]. Short overviews about the synthesis of glycerol oligomers from

di- to pentaglycerol have been published by Rollin *et al* [28]. Generally oligoglycerols are produced using basic homogeneous catalysis, but lately increased attention has been paid towards the heterogeneously catalysed processes. Despite a lower activity heterogeneous catalysts reveal many advantages: firstly, the separation of the catalyst and secondly, by carrying out the reaction in the absence of solvent, in this work only filtering the catalyst was needed, with evident economic and environmental advantages.

The conditions used for glycerol etherification were chosen with basic catalysis, since the sunflower oil production agriresidue derived materials (RP45), given their composition of alkaline (26 % potassium) and alkaline-earth cations (5 % magnesium and 7 % calcium) are basic in nature. TGMS of adsorbed acetic acid indicated that RP45 contained basic centres of low (100-200 °C), medium (200-500 °C) and high basicity (550-650 °C) (Figure 7) (see procedure for basicity measurement in reference 14) and can catalyse Knoevenagel condensation reactions [29].
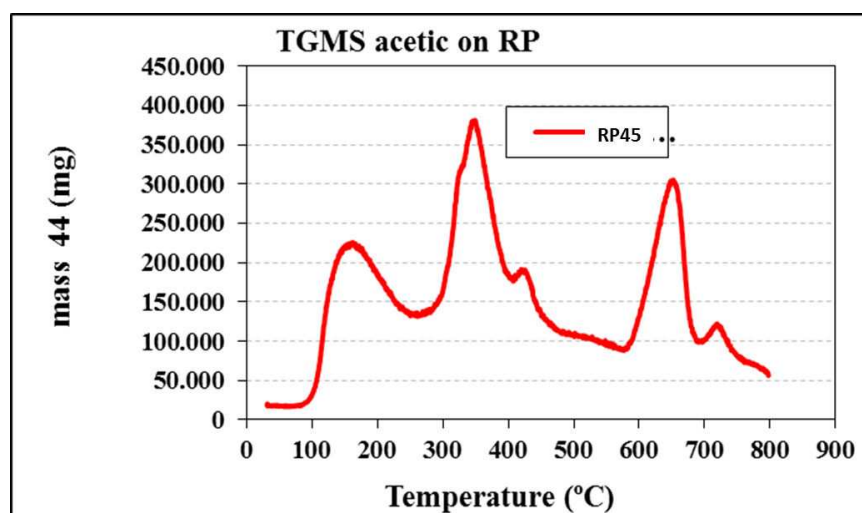
Figure 7. Analysis of basicity of RP45 by TG-MS of acetic acid decomposition.

The reactions were carried out in abscense of solvent, under inert atmosphere to limit over-oxidation, controlling temperature and time of reaction to optimise the economics [30, 31]. The work described here was carried out to produce diglycerol ethers in the absence of solvent, under inert atmosphere to avoid overoxidation, using catalysts derived from sunflower oil production residues, which have medium and high basic strengths. The analysis of reaction products was carried out by GC-MS (conditions as in reference 14).

Optimisation of the reaction conditions (Figure 8) showed that with 240°C, under inert atmosphere (nitrogen flow) and a ratio catalyst/glycerol = 1/50, after 4 h the conversions of glycerol and selectivities to diglycerols were optimum. At lower temperatures the conversions were low and with higher temperatures the selectivity to diglycerols decreased due mainly to uncontrolled formation of polyglycerols and oxidised compounds (mainly glycolic and glyceric acids).
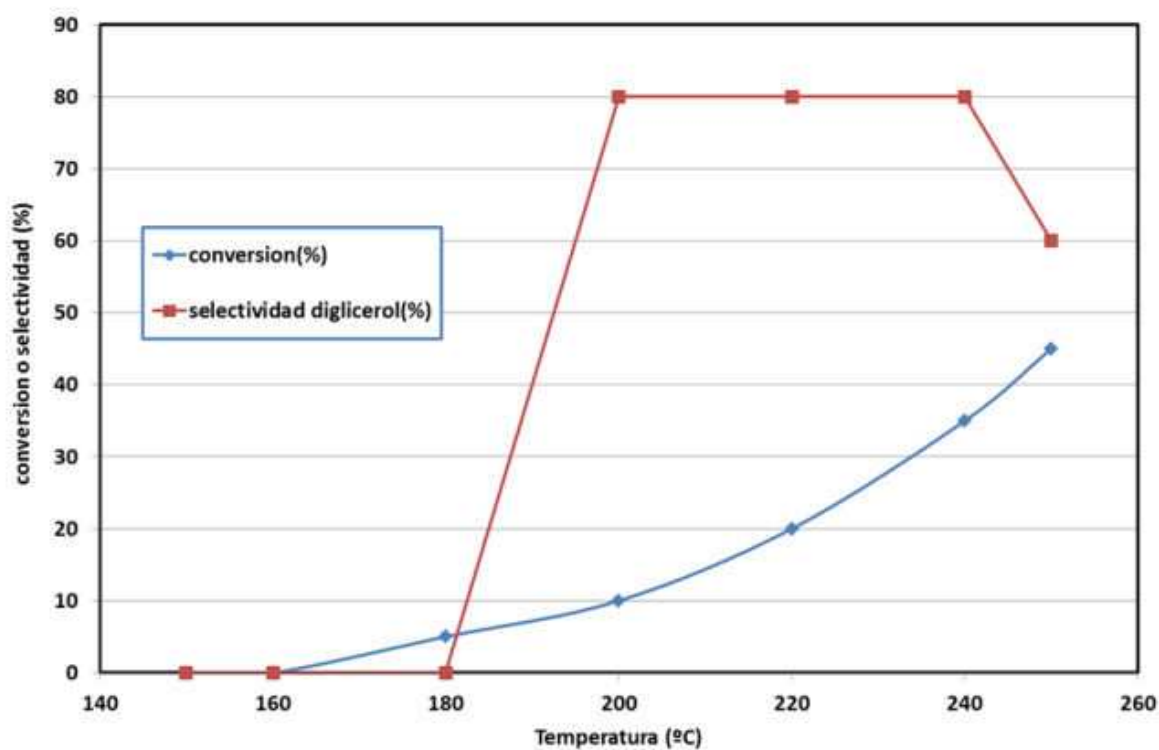
Figure 8. Conversions and selectivities of glycerol to diglicerol at different reaction temperatures.

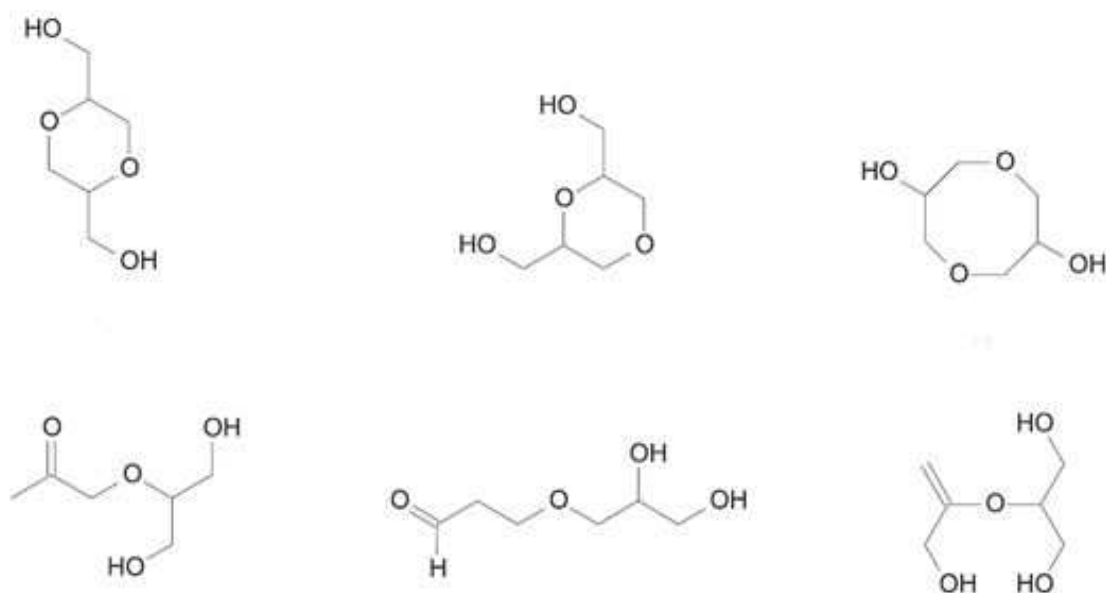Main compounds found in the reaction carried out in this work are summarised in Figure 9.

Figure 9. Main diglycerol ethers found in the present work.

The catalyst chosen for reference was sodium hydroxide, which was dissolved in the glycerol, where from the bibliography the amount of NaOH was chosen to give a molar ratio NaOH/Glycerol = 50 [32]. The homogeneous reaction with diluted NaOH (1 g/50 mls glycerol, 240 °C), reached 20 % conversion with glycerol ethers mainly cyclic (18-20 min analysis) after 3 h of reaction, lower temperatures gave very low conversions and higher temperatures or times decreases the selectitivty to diglycerol ethers due to unwanted triglycerol compounds (Figure 10). The reaction with RP45 (1 g/50 mls glycerol) led to a ratio between linear/cyclic diglicerol of 1/4, while on using homogeneous reaction, only cyclic diglyerol was produced under the conditions used (Figure 9). On increasing the NaOH/Glycerol or RP45/glycerol ratios the selectivity decreased due to unwanted glyceric and glycolic acids due to over oxidation and triglycerols [33].
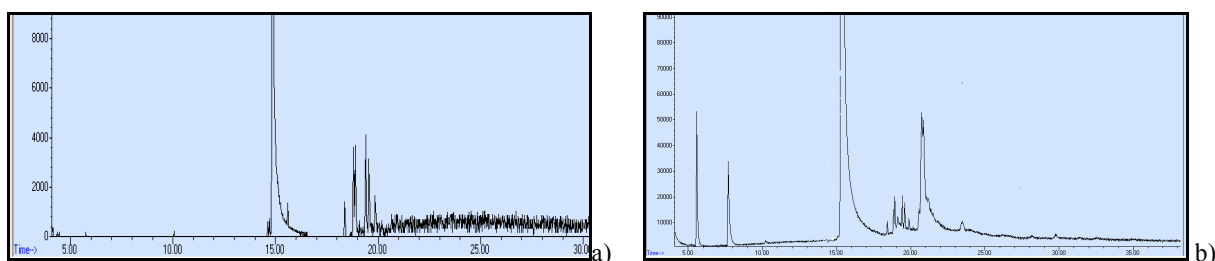
Figure 10. a) Homogeneous reaction of glycerol with NaOH (15 min glycerol, 18-20 minutos cyclic diglycerols). b) Activated RP45 (4 h reaction, 5.7 min: glycolic acid, 7.8 min: glyceric acid, 15 min: glycerol, 18-20 min: cyclic diglycerols, 21 min: linear diglycerols, 23 min: triglycerols).

Given the basicity of RP45 (see Figure 7) it carbontaes easily in the open atmosphere due to reaction with CO_2, therefore it was important to activate this material *in situ* to optimise its activity as a basic catalyst. This was done by heating to 500°C, reaching conversions close to 30 % after 6 h of reaction with selectivity to linear diglycerols close to 50 %. Also, the use of an inert atmosphere was necessary to avoid over oxidation [34]. The reactions carried out with RP47 and RP48 gave very low conversions as corresponds to their smaller active surfaces, since they were prepared at 700 °C and 850 °C respectively (RP47: 8 h, 5 % conversion, 75 % linear diglicerol, 25 % cyclic, RP48: 8 h, 2 % conversion, 50 % cyclic, 50 % linear) [20, 23, 31].

4. Lipases immobilised on materials prepared with agriresidues derived from rice production.

Lipases are enzymes of the hydrolases family, with capabilities such as hydrolysing triglycerides to diglycerides, monoglycerides, fatty acids and glycerol, by reaction of the carboxylic ester bonds. More than 25 % of enzymes used in biotransformations are lipases. However, their high production cost are their main disadvantage for industrial uses like soap and detergent production, baby milk preparation, hydrolysing the grease in milk or production of pharmacological substances. In the human body these substances are important since they facilitate fats adsorption.

Lipase immobilisation is of interest since it allows their reuse and increases their resistance to inactivation. For industrial applications, several properties are important *i.e.* mechanical strength, chemical and physical stability, hydrophobic/hydrophilic character, amount of immobilised enzyme and cost. The use of agroindustrial residues to prepare supports for immobilisation of enzymes can reduce the cost and therefore extend the use of lipases to an industrial scale, since these materaials are cost effective if the technology to make them competitive with commercial ones is developed. In this work the materials used to support enzymes where derived from rice husk (RH) and sunflower (RP) industrial production [13, 35].

The thermal stabilities of the residues in air were analysed by thermal techniques (TGA–DTA) on a Netzsch 409 EP Simultaneous Thermal Analysis device. Approximately 20–30 mg of powdered samples were heated in an air stream of 75 mLmin^{-1} at a heating rate of 5 °Cmin^{-1} from ambient to *ca.* 1000°C, using α-alumina as a reference. The termal data were used to design the controlled thermal treatments to produce agriresidue derived materials at temperatures between 500-700 °C, where the organic matter had been decomposed. The microstructure of the agriresidue derived materials was observed by scanning electron microscopy (SEM) (Hitachi S-4700 type I, Japan). (Figure11).
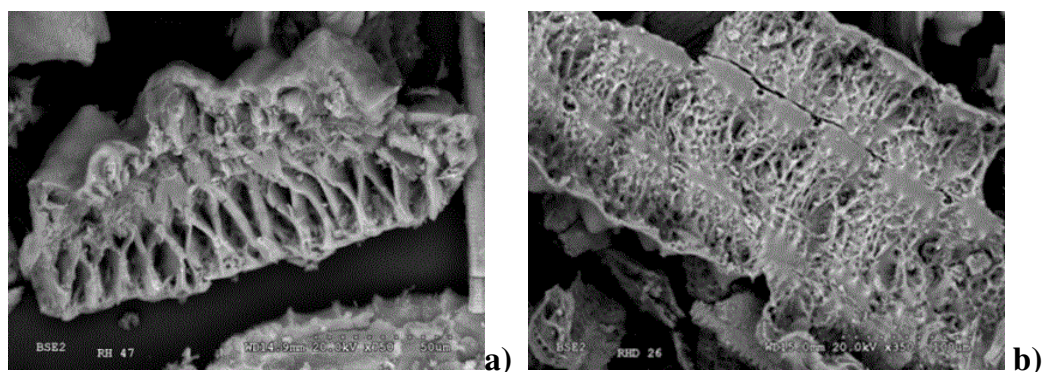
Figure 11. SEM images of rice production derived materials. a) RH47 b) RH26

The TXRF analysis of the materials derived from heat treated rice husk (RH47, RH45, RH26) indicated that they contain *ca.* 39 % silicon and 1-2 % calcium and potassium and those derived from sunflower production (RP45 and RP47) 14 % potassium, 12 % calcium, 7 % magnesium, 2 % phosphorous, 1 % iron and 1 % silicon.

The crystallinity of the materials was recorded by X-ray diffraction (XRD) on a Seifert 3000P diffractometer, using Cu Kα_1 radiation: λ = 0.15406 nm, at 2θ = 5-75 °, with 0.02 ° and 2 sec/pass (Figure 12). According to these analyses, the RH materials have amorphous structures as correspond to their siliceous nature with small amounts of alkaline and alkaline-earth cations. The materials derived from RP residues were crystalline solids with XRD patterns corresponding to oxides of potassium, calcium and magnesium when recently calcined, with increasing cristalinities on heat treatment, and their carbonates when in contact with CO$_2$ rich atmosphere (fairchildite (K$_2$Ca(CO$_3$)$_2$) (red lines), calcite (CaCO$_3$) (blue lines)).
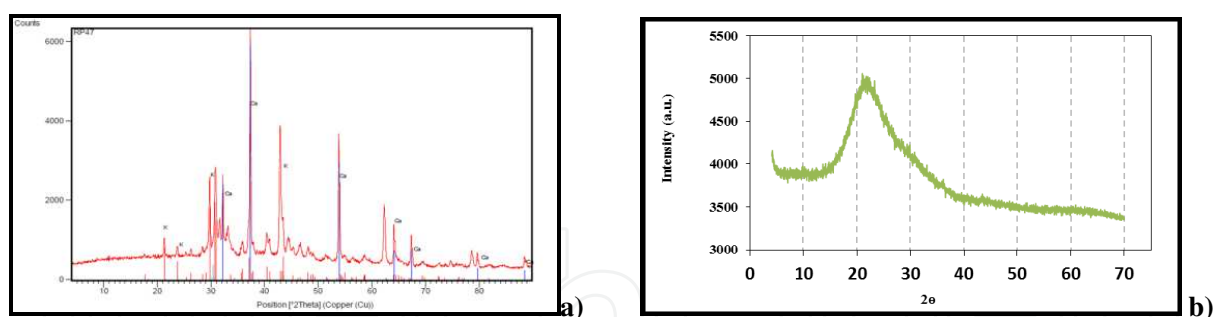
Figure 12. XRD patterns: a) RP47 b) RH26

Fourier transformed infrared transmission spectra (FTIR) of materials obtained on a Nicolet 40 FTIR spectrophotometer in the wavenumber range of 4000–400 cm^{-1}, using a 1/100 dilution in KBr indicated the presence of bands at 900-1200 cm^{-1} and at 400-600 cm^{-1}, corresponding to metal-oxygen bonds (800 cm^{-1} is O-Si-O symmetric stretching vibrations), given the oxide structure of the materials freshly calcined and bands of OH- at *ca.* 2900-3500 cm^{-1}, that decrease on increasing the treatment temperature due to the loss of water from the OH- groups, carbonate groups are found at 1400-1460 cm^{-1} and bands close to 2100 cm^{-1} corresponding to C=O groups present in organic matter, that decrease with the treatment temperature.

The specific surface areas measured by N_2 adsorption at 77 K after outgassing overnight at 150 °C and employing the BET method for data analyses in a Sorptomatic 1800 instrument (Table 4) indicated that RH derived materials are mesoporous with type IV isotherms and wide pore size distributions, and RP derived materails are non-porous with type II isotherms and non-existent hysteresis loops. Specific surface areas are listed below.

Material	SBET m^{2}g^{-1}
RH26	63
RH45	98
RH47	16
RP25	8
RP47	4

Table 4. Textural analyses by N_2 adsorption desorption and BET calculations

The porosities in pores from 300 μm down to 7.5 nm were determined by mercury intrusion porosimetry (MIP) using CE Instruments Pascal 140/240 porosimeter on samples previously dried overnight at 150 °C, the Washburn equation was employed, assuming a non-intersecting cylindrical pore model and the recommended values for the mercury contact angle and surface tension of 141 ° and 484 mNm^{-1}, respectively. These studies show that materials RH26 and RP47 have pore volumes, mesopores areas, medium pore radii and medium particle sizes as

follows: RH26 (0.08 cm^{3}g^{-1}, 27 m^{2}g^{-1}, 80 μm and 90 μm), RP47 (0.02 cm^{3}g^{-1}, 4 m^{2}g^{-1}, 15 μm and 30 μm).

In order to measure the basicity of the solids acetic acid was previously adsorbed onto the powder materials and subsequently the mas of 44 was recorded against temperature with a quadrupole mass spectrometer, M3 QMS200 Thermostar coupled to Stanton STA model 781 TG/DTA apparatus. For these analyses approximately 50 mg of the materials were dosed with acetic acid, transferred to the crucible placed within the Stanton TG-MS, where they were subsequently flushed with nitrogen gas at room temperature in order to desorb any loosely bound physically adsorbed acetic acid, until a constant weight was attained. The decomposition of the chemisorbed acetic entities was then achieved by increasing the temperature under a nitrogen flow at a heating rate of 5 °Cmin^{-1}.

The amount and temperature of evolution of the CO_2 signal gave an indication of the strength and amount of basic sites. The CO_2 signal was calibrated from the decomposition of a known amount of calcium oxalate. These measurements indicated the presence of basic groups of high (>500 °C), medium (300-500 °C) and low basicity (100-300 °C) for RP materials, as corresponds to their content in alkaline and alkaline-earth cations and the RH materials had lower amounts of basic centers and of lower strength than the RP materials (Figure 13) [14].
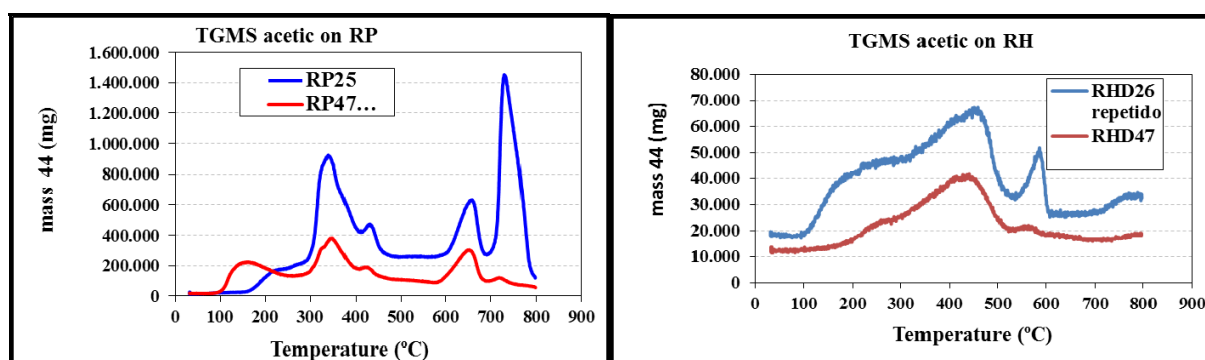

**Figure 13.** TGMS acetic acid decomposition on RP or RH derived materials.

The immobilisation process and measurement of activity was undertaken until there was no significant variation in activity. Subsequently, the biocatalyst was filtered, washed, dried over P_2O_5 and the enzymatic activity was studied at 30 °C, using a Mettler Toledo (modelo DL-50) pH-stato at pH=8.0 with 0.1 N NaOH titrating agent. As reaction medium 19 mL of 1nM tris-HCl buffer at a pH 8.0, 0.6 mL of acetonitrile and 0.4 mL of tripropionine as reaction substrate. A blank test was done to measure spontaneous hydrolisis (without enzyme and only with the triglyceride and the reaction medum). This technique consists of the controlled addition of a basic solution to maintain the pH, being then the titration proportional to the production of acid and therefore to the reaction rate.

The enzyme immobilisation on RH materials indicated that during the initial hours the percentage of immobilised enzyme grows but after 24 h there was no more absorption, however, when RP materials were used there was a continuous increment of immobilised

enzyme, probably due to their lower pore volumes compared to RH materials. The materials that immobilised more enzyme were RH45 and RH26, where the latter was chosen for further studies since it had the highest catalytic activity. For the enzymatic activites, lipase Rhizopus oryzae expressed on levadura Pichia pastori, from the Autonoma University of Barcelona, was used. The lipase received as a solid was used to prepare the enzymatic solution of 20 mg/ml with sodium phosphate buffer 100 mM and pH 6.5, incubated stirring for 1 h at 4 °C and centrifuged to eliminate any solid residue [36].

The measurements of enzymatic activity, in sobrenadantes, control and stock solutions were carried out in a plate reader Versamax, using 10 mM p-nitrophenyl propionate (pNPP) as reaction substrate, in kinetic mode, with a wavelength of 405 nm, 30 °C and 2 min. Since the data are given in mU/min, the enzymatic activity was calculated with an extinción coeficient (ε) for the pNPP appropiate to the wavelength and pH, $\varepsilon = 16780$ M^{-1}cm^{-1}. The analyses of protein concentration was done by the Bradfor Method using the Biorad reactant and proce-dure, based on the capacity of dye *Comassie brilliant blue G-250* to change color in the maximum of absorption in the range 465 a 595 nm, according to different concentration of proteins (orange colour becomes blue on the dye bonding to protein at 595 nm. Calibration curves for this procedure were measured with a 50 μg/ml solution of bovine serum albumin (BSA) as standard.

The experiments to study the reactions of hydrolysis were carried out using different enzymes, the test reaction of biodiesel synthesis by transesterification of triglycerides (trilaurin or triolein, Figure 14) with metanol or etanol was done where the main products were ethyl or methyl oleate or laurate and as secondary products mono and diglycerides and the corre-sponding fatty acid due to triglyceride hydrolysis.
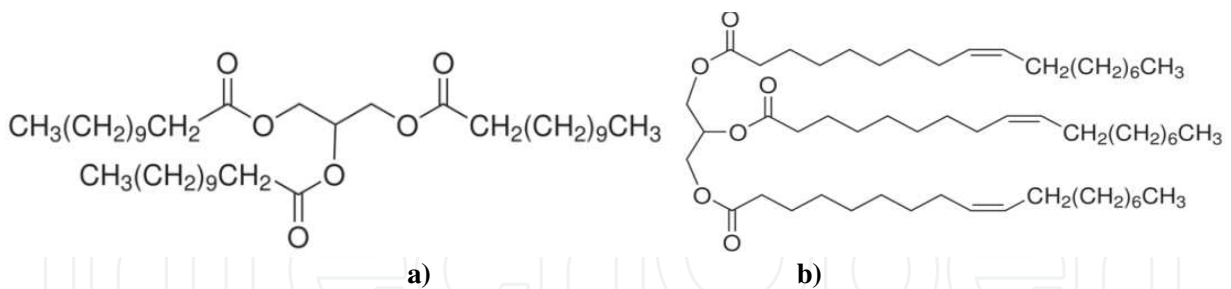
Figure 14. Trilaurin (a) and triolein (b) formulas.

Transesterification reactions were carried out with 50 mM ester concentrations and triglycer-ide:alcohol molar ratio 1:4, using 2-methtl-2-butanol (2M2B) as solvent, 20 mg/ml of enzyme, 45 °C and 300 rpm stirring speed. The progress of reaction was quantified by means of TLC chromatography, using a solution of hexane, ethyl acetate and glacial acetic acid (90:10:1) and developed by a solution of etanol, water, glacial acetic acid and a dye (*Comassie blue*) (20:80:0.5:0.03) and HPLC composed of a quaternary pump Waters E600, an injector and photodiode detector Varian ProStar and a refractive index detector Waters 2410, with a *Cosmosil* C18 of 4.6 x 150 mm column with a medium particle size of 4.4 μm, at 40 °C with a

mobil phase of metanol and water acidified with 0.1 %V acetic acid and variable methanol:water ratio. The analysis method is based on time gradient, varying composition and flow of the mobil phase until only methanol is passed.

Transesterification of triglycerides with methanol and ethanol produce mainly methyl and ethyl oleate and secondary compounds such as fatty acid esters (mono- and dilaurin, mono-olein and diolein) and the corresponding fatty acid due to the triglyceride hydrolysis. On using Novozym 435, trilaurin disappears after 24 h of reaction, because when the trilaurin is consumed, ethanol interacts with the diglyceride. Regarding the use of Lipozyme TL-IM, ethyl laureate formation is slower, although trilaurin also gets consumed and the formation of acid is lower, because Lipozyme TL-IM has a lower amount of water than Novozym 435. In the case of Lipozyme RM-IM, the formation of ethyl laureate is not so important as in the cases stated before, and at 24 h there is still a lot of unreacted trilaurin.

Sample	Immobilised Enzyme (%)	Catalytic Activity (U/g)	Recovered Activity (%)	S_{BET} (m^2g^{-1})
RH45	60	393.5	28	98
RH47	46	671.5	60	16
RH26	57	737.2	53	63
RP45	39	308.1	22	8
RP47	49	67.0	4	4

Table 5. Textural and reactivity data for enzyme immobilised on agriresidue derived materials.

Amongst the materials used, those derived from rice husk show higher capacities for lipase absorption. It should be noted that RH45 and RH26 are the materials that have highest surface areas, but taking into account the amount of enzyme absorbed, it is clear that not only the textural characteristics are defining the behaviour of the supports but the amount and strength of the basic sites was also important, much higher in the RP materials. RH26 was chosen for preparation of immobilised enzyme for biodiesel synthesis in comparison with commercial enzymes. The ROL enzyme supported on RH26 prepared in the group had a higher activity than Novozyme 435 and similar to that of Lipozyme TL-IM, both lipases widely used in biocatalysis. Trilaurin was consumed in *ca.* 24 h with ethyl laureate formation close to that of Novozyme 435 and lauric acid due to the hydrolysis produced by the water contained in the enzyme.

	RH26	Novozyme 435	Lipozyme TL-IM	Lipozyme RM-IM
U/g	1347.2	1321.5	1444.5	95.4

Table 6. Comparison of reactivity of commercial and agriresidue supported enzymes.

The biocatalysts prepared by immobilisation of the lipase on agriresidue derived materials, given their renewable origin and low cost, seem to be an attractive option for reducing costs and environmental impact of these processes [37, 38].

5. Bioecomaterials

5.1. Tissue engineering (Dental and Bone replacement therapies)

Bone tissue engineering is one of the most promising approaches to be used as an alternative to conventional autogenic or allogenic surgical techniques for bone tissue repair [39]. Bone grafts are used to stimulate the formation of new bone in many conditions such as congenital anomalies, cancers, and trauma or to improve the regeneration of bone tissue around surgically implanted devices.

An ideal bone graft or scaffold should be made of biomaterials that emulate the structure and properties of natural bone extracellular matrix providing all the necessary environmental cues present in natural bone. The tissue regeneration capacity of these bone grafts is measured in terms of their osteogenic, osteoconductive and osteoinductive potential. The osteogenic potential of a bone graft is given by cells involved in bone formation, such as mesenchymal stem cells, osteoblasts, and osteocytes. The term osteoconductive refers to the scaffold or matrix which stimulates bone cells to grow on its surface. Osteoinductive capacity of a bone graft is perhaps the most important property in bone healing as it refers to the stimulation of mesenchymal stem cells to differentiate into preosteoblasts to begin the bone-forming process [40].

A possible therapy for the treatment of skeletal defects has arisen with the use of synthetic materials as bone substitutes. Tissue engineering strategies based on the use of biocompatible and biodegradable porous materials that act as structural templates or scaffolds to guide the growth and development of new bone tissue, supporting both extracellular matrix formation and cell-cell interactions [41]. Due to their similarity to the chemical composition of bone, calcium phosphates can be used to regenerate osteoporotic bone as coatings that improve orthopedic implants, and for odontostomatologic applications, where their particle and crystal sizes are important parameters to be controlled to optimise these processes [42]. Calcium phosphate-based scaffolds exhibit osteoconductivity, bioactivity and resorbability *in vivo* due to their complex chemical composition (Ca/P ratio) and physical properties such as crystallographic structure and porosity [40]. However, major drawbacks in the use of synthetic calcium phosphates are their price and use of non-renewable resources.

Biomaterials based on composites of calcium phosphates and silica have the ability to bond directly to bone and thus enhance bone formation through supply of chemicals needed to support cell function and tissue formation. Furthermore, it has been found that addition of silica to the calcium phosphate scaffolds was beneficial in increasing the mechanical strength, cellular proliferation and dissolution/resorption rates [43, 44]. Moreover, the presence of magnesium in these materials favours bone growth, promoting osteogenic differentiation of preosteoblasts and improving osteointegration during the early stages of bone healing. During

the *in vivo* degradation of the scaffolds cell proliferation and differentiation are promoted by the release of their component elements [45-47].

With the aim to convert waste into value-added products agricultural wastes (such as beer bagasse) have been investigated as potential renewable raw materials to develop bone scaffolds capable to support osteoblast growth for bone regeneration applications. Materials prepared here with residues from beer production contain P, Si, Ca and Mg as main components, which are also cations present in bone [11, 48]. Furthermore, the use of agricultural wastes to provide renewable raw materials for more advanced applications is of great interest giving value-added products that may lead to a significant reduction in waste accumulation. Moreover, due to their origin these materials are very competitive in price [49]. The materials derived from beer bagasse (BBM) were biphasic calcium-magnesium phosphates with silica that can be either amorphous or as cristobalite, its crystallinity increasing in accordance with the final heat treatment temperature employed, with porosities that lie within the 10 to 100 μm range. All of these characteristics were important for the promotion of both cell proliferation and differentiation [50].

Osteogenic cells MC3T3-E1 are widely employed to study *in vitro* matrix mineralisation, since these cells can differentiate into osteoblasts that express strong ALP activity and can form a collagenous matrix organised in 3-dimensional nodules, which in the presence of ascorbic acid and phosphate progressively become mineralised [51]. The MC3T3-E1 cells display a time-dependent sequential expression of osteoblast characteristics that are analogous to *in vivo* bone formation [52]. It has been shown that some biomaterials are able to modify directly the osteoblastic proliferation rate and its differentiation, such as the synthesis of alkaline phosphatase, matrix mineralisation and collagen secretion [53,54]. Thus, the *in vitro* proliferation and differentiation responses of this osteoblast like cell line (MC3T3-E1) to the BBM derived powders were studied. Several biological responses to the biomaterials were assayed, including determinations of cell viability by the MTT and LDH assays, evaluation of ALP activity, Type- I collagen secretion and evaluation of matrix mineralisation at the differentiation period.

The present work employs residues from beer production from three different Spanish plants, Lerida, Guadalajara and Burgos from the Mahou San Miguel group. These residues were chosen so that a comparison of their suitability and any effects of the differences in their chemical compositions on their cytocompatibility for bone growth could be determined. The beer bagasses were first dried at 150°C for 4 h, at a heating rate of 5 °C/min, in order to avoid putrefaction, due to their high humidity (70–85 wt%). Thermal stabilities of the dried materials were determined by TG-DTA analyses in air, to assess the temperature necessary to eliminate the organic matter and prepare stable and reproducible materials. Results from TG-DTA indicated that the thermal behaviour of the three samples under air treatment was practically identical, with total weight losses found of *ca*. 97 % of the initial mass, 8 % due to loss of volatile matter and water at T < 200 °C, 55 % loss at T = 200-380 °C caused by the decomposition of organic matter (mainly cellulose and hemicellulose) and finally a 34 % lost for T = 380-600 °C, corresponding to the decomposition of lignin [48,49]. For a more detailed explanation the results obtained with sample BBM Lerida are shown in Figure 15b.
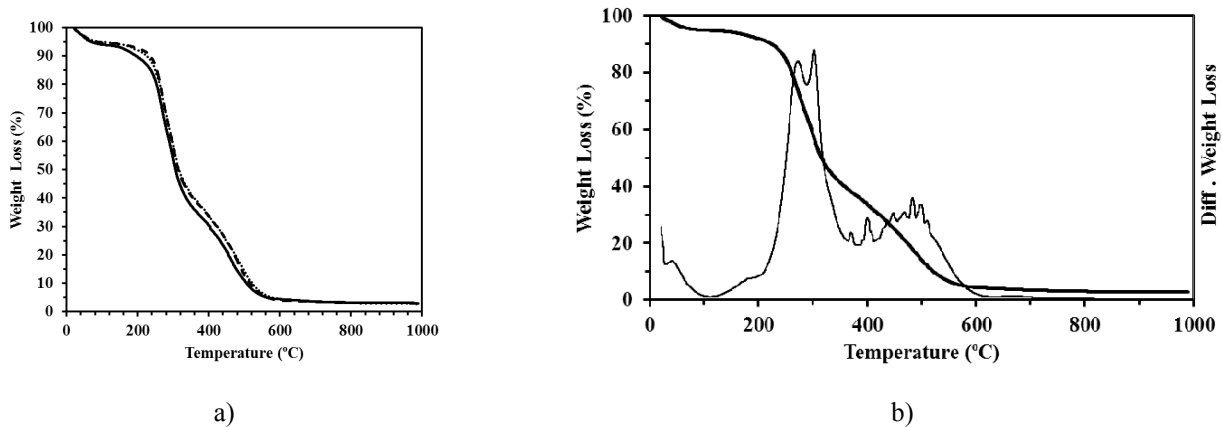
Figure 15. Reproducibility of beer bagasse from a) Lerida, Guadalajara and Burgos and detailed analysis of b) BBM-Lerida.

The samples of bagasse were then calcined at 600, 700, 850 or 1000 °C, maintaining the final temperature for 4 h, the samples thus produced were designated as BBM46, BBM47, BBM48 and BBM410, respectively. The calcined materials were homogenised and their particle sizes controlled by being milled to less than 120 μm, due to the importance of this parameter in the reproducibility of biological behaviour of the materials.

The composition of the calcined materials was analysed by means of inductively coupled plasma atomic emission spectroscopy (ICP), showing four main elements that depending on the source of the beer bagasse were 15–20 % silicon, 12–14 % phosphorous, 7–8 % calcium and 5–7 % magnesium. The variations between different batches of beer bagasse from the same source were negligible and within experimental error. X-ray diffraction (XRD) patterns of samples showed that with higher heat-treatment temperatures the XRD peaks were narrower and better defined due to the increased crystallinity of the materials. The most significant crystalline phases were calcium-magnesium phosphate (*) (31.5 ° (100 %), 29.7 ° (85 %) and 29.3 ° (75 %)) present at all temperatures and cristobalite which was only found when heat treatment temperatures greater than 600 °C were employed (21.9 ° (100 %, (111)), 36 ° (12 %, (220)), 31.3 ° (10 %, (102)) and 28.4 ° (8 %, (111)) [50, 51].

No crystalline cristobalite was found for BBM46 but mean crystallite sizes of 56 to 70 nm, 60 to 85 nm and 85 to 230 nm were found for BBM47, BBM48 and BBM410, respectively (Figure 16).

The three beer bagasses as received had identical FTIR traces and the heat treated materials prepared from them also displayed identical results. For the bagasse dried at 150 °C the principal bands were due to a broad band of O-H stretching in the 3100-3600 cm^{-1} region, the C-H aliphatic axial deformation in CH_2 and CH_3 groups from cellulose, hemicellulose and lignin at 2926 cm^{-1}, the -OCH_3 vibration at 2854 cm^{-1} due to lignin or hemicelluloses. The C=O stretching of the acetyl groups present in cellulosic material at 1743 cm^{-1}, while the bands at 1043 and 1160, corresponded to O-H stretching of primary and secondary alcohols, respec-
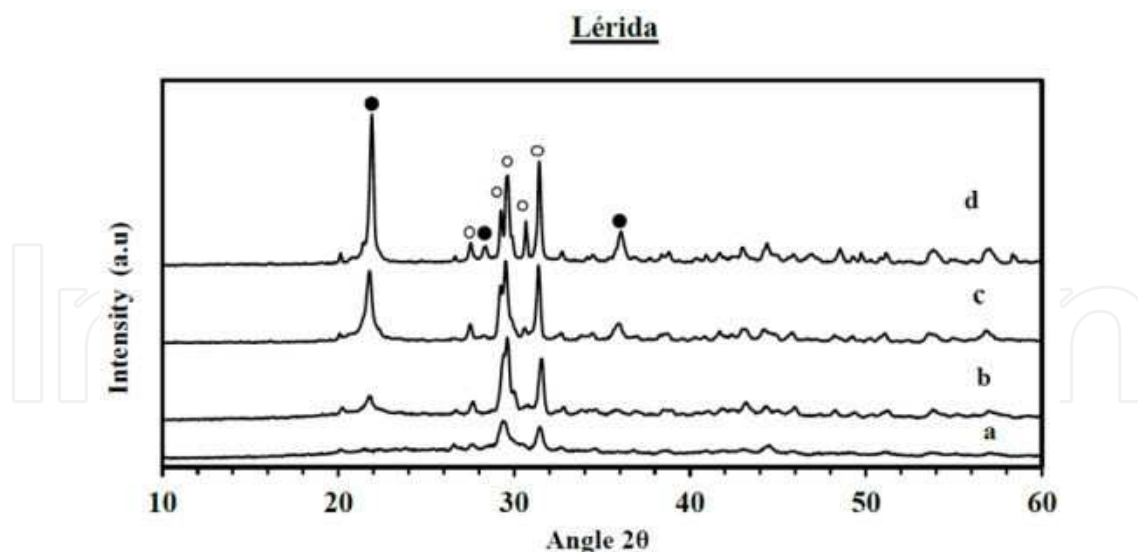
Figure 16. XRD patterns of Lerida agriresidue derived materials heat treated at 600 °C a, 700 °C b, 850 °C c and 1000 °C d.

tively and the band at 1378 cm^{-1} corresponded to O-H vibration of phenolic groups. The signal at 899 cm^{-1} was assigned to β-glycosidic linkages between monosaccharide units. For the heat treated materials the broad band at 3466 cm^{-1} was due to the stretching vibration of the P-OH and Si-OH groups that was diminished with respect to the dried materials due to the loss of these groups on heating. The bands at 1164, 1121 and 1097 cm^{-1} were due to the Si-O-Si asymmetric stretching vibration, a band at 470 cm^{-1} associated with a network O-Si-O bond bending modes. The band at 1023 cm^{-1} was attributed to the symmetric terminal P-O stretching mode of the calcium magnesium phosphate, a band for asymmetric bridge P-O stretching mode appeared at 964 cm^{-1} whilst those at 579 and 496 were due to the asymmetric bending vibrations of terminal P-O bands [52-54].

The porosities and particle size distributions of the heat treated materials were determined by Mercury Intrusion Porosimetry. From Figure 17 it may be appreciated that the majority of the intrusion curve was due to interparticulate pore filling and that only with the materials treated at the lowest temperature was there any sign of mesoporosity, pores with diameters lower than 50 nm, due to intraparticulate porosity, which due to sintering of the materials disappeared on heating at higher temperatures.

As the heat treatment temperature was raised the density of the materials increased with a corresponding reduction in the cumulative pore volume accompanied by a slight displacement of the curves to wider pores. For finely divided powder samples the cumulative intrusion curve represents the void filling between the aggregates of the primary particles. Thus, an evaluation of their size may be made using the Mayer Stowe theory that relates the porosity of the sample to a packing factor, assuming spherical particle geometry, which is used to estimate the particle size from the measured width of the spaces between the particles. It may be observed from the results that higher heat treatment temperatures caused an increase in the aggregate sizes and a densification of the materials due to sintering of the samples, which was in agreement with the results observed from the XRD analyses of these materials [55,56].
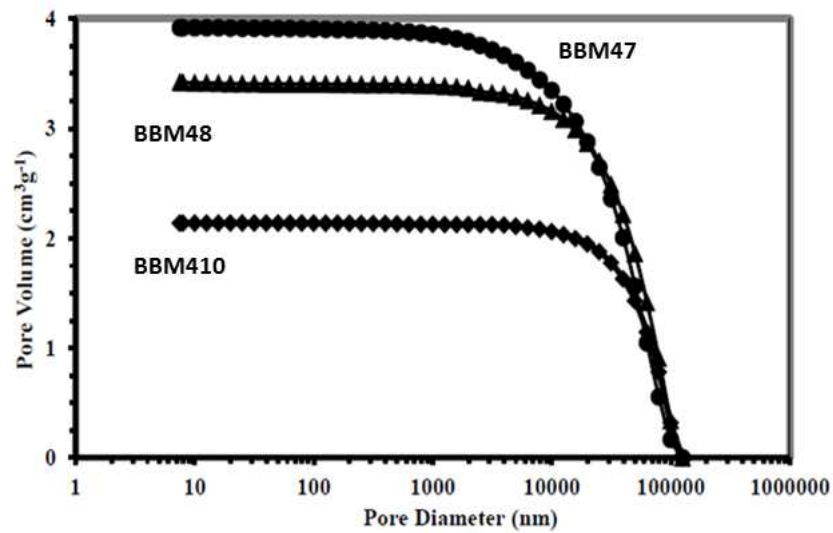
Figure 17. Mercury intrusion porosimetry results for beer bagasse from Burgos treated for 4 h at 700 °C, 850 °C or 1000 °C.

Analyses of the basic character of materials by decomposition of acetic acid (Figure 18) indicate higher amount of basic sites for those prepared at lower temperatures, agreeing with the sintering process observed by the other characterisation techniques.
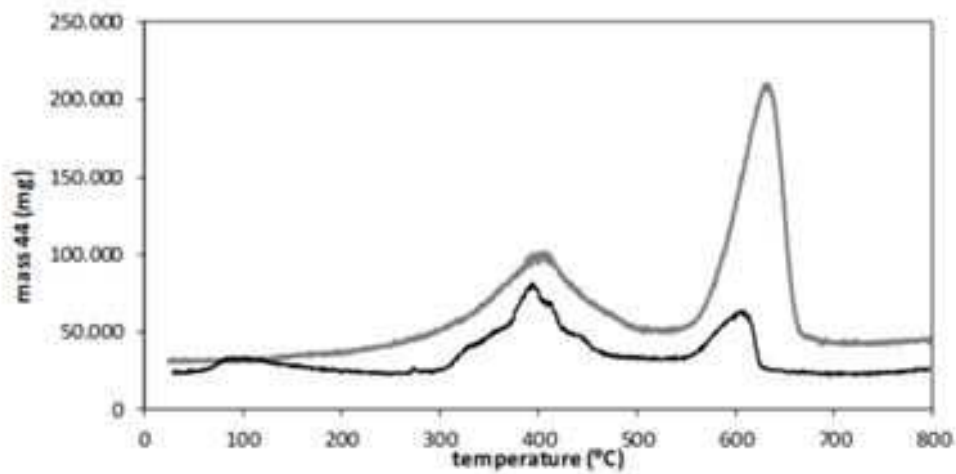

Figure 18. TGMS analyses of decomposition of acetic acid on BBM47 (grey line) and BBM410 (black line).

### Cell proliferation and differentiation on BBM derived materials

Cell cultures

The osteoblast-like MC3T3-E1 murine cells were cultured in α-MEM (Gibco) that was supplemented with 10 % foetal bovine serum and 1 % penicillin-streptomycin (basal medium). In order to induce differentiation the cells were placed in osteogenic media: a basal medium supplemented with 10 mM β-glycerophosphate and 50 µg/mL ascorbic acid. These cells were

incubated at 37 °C in a humidified atmosphere and at 5 % CO_2. The cell culture results obtained were compared with a reference material, hydroxyapatite (HA), a synthetic calcium phosphate ceramic that mimics the natural apatite composition of bones and teeth and has been described as a potential material to coat scaffolds for promoting osteoblast differentiation [55,56].

Cell proliferation on BBM derived materials

Cell proliferation assays were performed in the presence of increasing concentrations of BBM derived materials from Lerida, Guadalajara and Burgos treated at increasing temperatures, after culturing cells in basal medium for 7 days, in order to determine the influence of the origin of the bagasses and the effect of the temperature to which they were subjected. To evaluate the proliferation rate of MC3T3-E1 cells grown in the presence of BBM derived materials, the cell viability was measured following incubation of the cells with materials at various concentrations, ranging from 20-200 μg/mL for 7 days. HA was used at the same concentrations as a reference material. To carry out the viability assays the cells were seeded into 96-well plates (10000 cells per well; four replicates for each condition). After 24 h, the cells were treated with materials for the specified concentrations and time periods. The cultures were then washed twice in phosphate buffered saline to remove any residual material. Subsequently, the tetrazolium dye, 3-(4,5-dimethilthiazol-2)-2,5-diphenyl-2H tetrazolium bromide (MTT, 5 mg/mL in phosphate-buffered saline; Sigma), was added to the medium and left for 1 h. Following removal of the medium, the precipitated formazan crystals were dissolved in optical grade dimethyl sulphoxide (200 μL). Then by use of an ELX808 microplate reader (BioTeK) the absorbance of each well was measured spectrophotometrically at 570 nm. When beer bagasses were treated at lower temperatures a decrease in cell proliferation rates was observed (Figure 19).
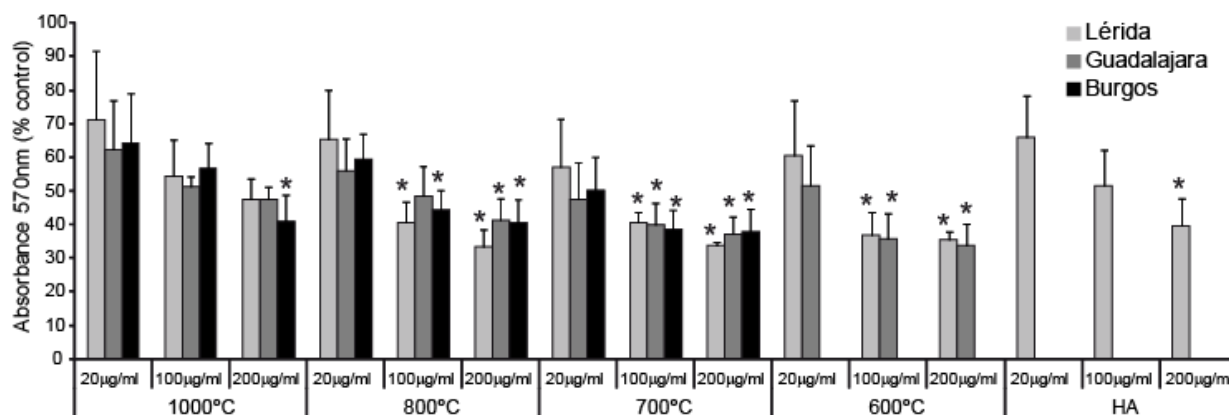
Figure 19. MC3T3-E1 proliferation analysis by MTT assay on cells treated with different concentrations of BBM derived materials treated at several temperatures after one week in culture. The data were analysed by single factor analysis of variance followed by the *post hoc* Tukey's honestly significant difference test, *p<0.05 with respect to control (cells growing on polystyrene plates).

We found that the addition of BBM derived materials to MC3T3-E1 cells did not considerably alter the viability of the cells, compared to the reference material (HA). When BBM derived materials were subjected to 1000 °C for 4 h, proliferation analysis assessed by MTT test showed

a similar cell growth to that obtained when using HA as reference material. However, a decrease in cell proliferation rates was observed when BBM derived materials were treated at low temperatures (600 °C). The observed delays in cell proliferation were due to the more basic pH for the powder containing media at the first day in culture, which could initially result in a lower cellular enzymatic efficiency and hence in slower processes (e.g. cell division and metabolism) than that observed with the control cells, growing on polystyrene plates [57]. The different relative metabolic levels found in MC3T3-E1 cells growing in the presence of BBM derived materials at day 7 also correlate with the characteristics of the powders, where materials pretreated at lower temperatures produced higher increases in the pH of the culture medium due to their greater basicities, leading to lower proliferation rates of the MC3T3-E1 cells.

According to these findings, further cytotoxicity assays and cell differentiation experiments were performed on the BBM derived biomaterials treated at 1000 °C.

Cytotoxicity

The cytotoxicity of the culture media was related to the lactate dehydrogenase (LDH) activity. The measurements were determined on cells plated at a density of 10 000 cells per well in 96-well plates in basal and osteogenic medium. Beer bagasse materials treated at 1000 °C for 4 h were added at 100 μg/mL. After 24 h, the culture media were collected and centrifuged and the supernatant was used for the LDH activity assay. The LDH activity was determined spectrophotometrically using the Cytotoxicity Detection kit (Roche), according to the manufacturer's instructions. Cells cultured in the presence of BB-derived materials showed no obvious cytotoxicity compared to cells grown in the presence of hydroxyapatite and polystyrene culture plates, used as controls (Figure 20).
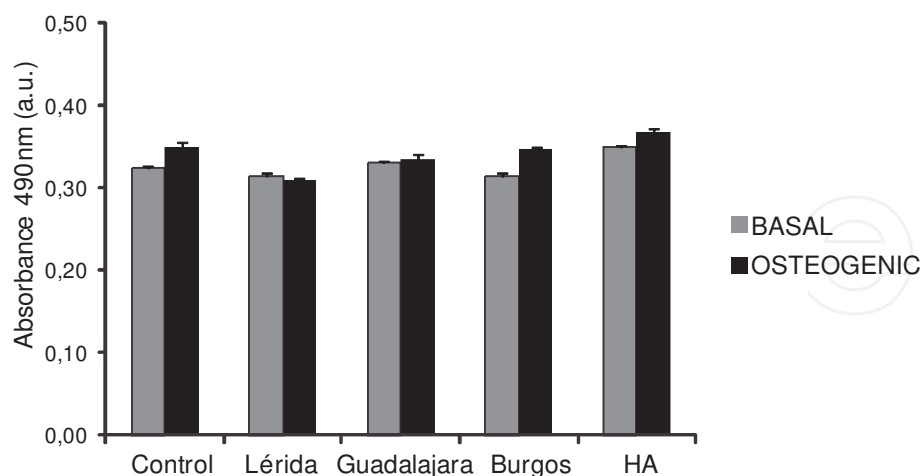
Figure 20. Cytotoxicity study by lactate dehydrogenase (LDH) activity assay on MC3T3-E1 cells treated with 100 μg/ml of BBM derived materials treated at 1000 °C and HA, after 24 h in culture.

Results obtained in LDH assay when MC3T3-E1 cells were cultured in the presence of BBM derived materials for 24 h support the cytocompatibility of these new materials.

Cell differentiation

Previous studies have demonstrated that expression of osteoblastic markers in MC3T3-E1 cells begins after culturing the cells with medium supplemented with β-glycerol-phosphate and ascorbic acid [52]. The effects of direct contact of BBM derived materials and osteoblast-like cells in terms of cell differentiation were evaluated by testing alkaline phosphatase (ALP) activity, collagen production and extracellular matrix mineralisation after 15 days in culture. Alkaline phosphatase activity (ALP) begins to be expressed after 1 week and reaches a maximum after 2 weeks when MC3T3-E1 cells are cultured in osteogenic medium [52].

The capacity of cells growing in the presence of BB-derived materials was evaluated to express alkaline phosphatase, an early marker of osteoblastic cell differentiation. To this end, MC3T3-E1 cells were seeded into 96-well plates (10 000 cells per well; four replicates for each condition) and grown on basal and osteogenic medium for 15 days in the presence of BB-derived materials at 100 µg/ml. After treatment with the BBM derived materials, the cells were rinsed with PBS and then lysed into PBS containing 0.1 % Triton X-100. These cell lysates were then centrifuged and the soluble fraction used for the enzyme assay. The samples were first incubated with an assay mixture of p-nitrophenyl phosphate (p-NPP) (Sigma). Cleavage of the p-NPP in a soluble yellow end product, p-nitrophenol, which absorbs at 405 nm, was used to assess the ALP activity. The optical density of p-nitrophenol at 405 nm was then determined spectrophoto-metrically and the ALP activities normalised to total protein content using the bicin-choninic acid (BCA) method. The ALP activity of each condition was quantified and compared to that present in cells grown on polystyrene plates used as the (control).

It was found that the ALP activity was higher in cells grown in osteogenic medium than for cells cultured in basal medium, as we would predict (Figure 21). However, there was no significant difference in the ALP activity observed for MC3T3-E1 cells grown in the presence of HA and with control cells. These results established that the presence of BB-derived materials did not affect ALP activity.
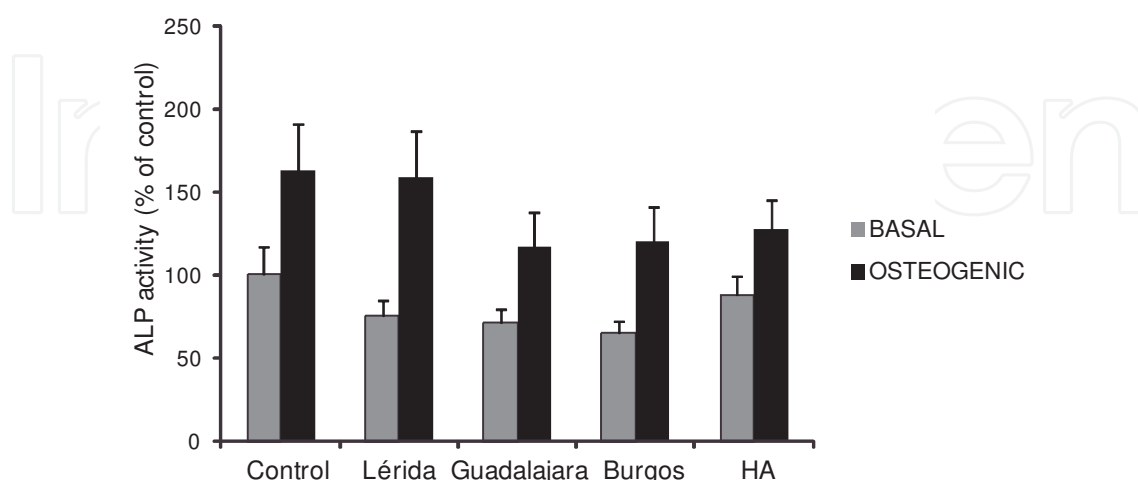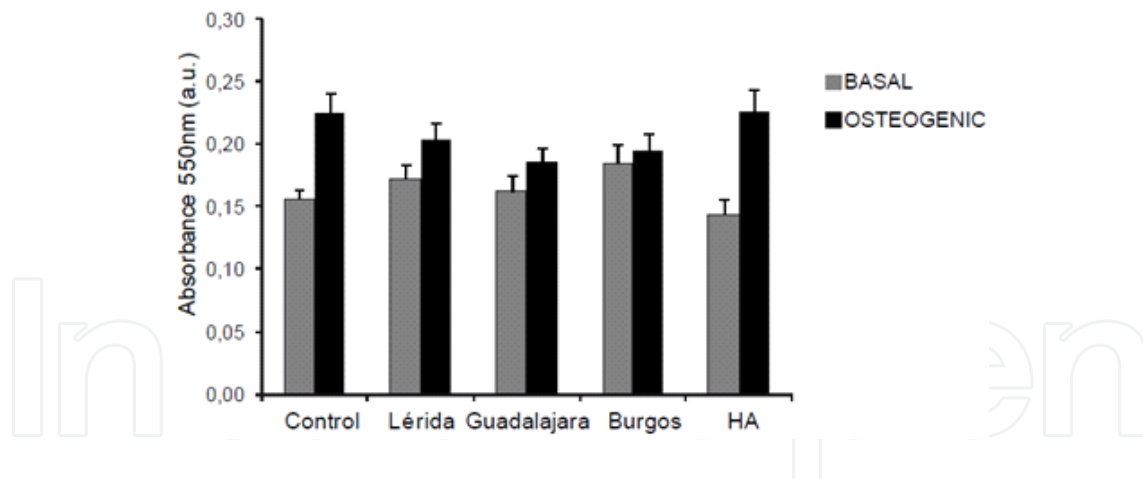

Figure 21. MC3T3-E1 differentiation study by alkaline phosphatase (ALP) activity assay on cells treated with 100 µg/ml of BB-derived materials and HA after 2 weeks in culture.

Results indicated that MC3T3-E1 cells maintain their capability to express active ALP enzymes when growing in the presence of BBM derived powders.

The addition of ascorbic acid in MC3T3-E1 cells is known to induce the deposition of collagen in the extracellular matrix [52]. To confirm that osteoblastic cells exposed to the BB-derived materials indeed maintained the ability to differentiate at similar levels to control cells, the profile of type-I collagen cellular secretion, the main extracellular matrix protein expressed in bone, was also analysed. Collagen secretion by MC3T3-E1 cells cultured in the presence of BB-derived materials treated at 1000 °C for 4 h, at 100 μg/mL was quantified by Sirius Red staining. After culturing MC3T3-E1 cells in the presence of BB-derived materials for 15 days in both basal and osteogenic media, the cells were washed three times with PBS and then fixed in 4 % paraformaldehyde. Following the three rinses in PBS, the cell cultures were stained for collagen secretion in a 0.1 % solution of Sirius Red (Sigma) in saturated picric acid for 18 h. Following washing with 0.1 M acetic acid until the disappearance of the red colour, the stain on specimens was eluted in destain solution (0.2 M NaOH–methanol 1:1). The optical density at 540 nm was then determined using a spectrophotometer.

From the results shown in Figure 22, it may be seen that collagen deposition was promoted when MC3T3-E1 cells were grown in osteogenic medium at all the tested conditions, as expected and no significant differences in the collagen production were observed for cells grown in the presence of BB-derived materials compared with those grown on plastic plates, neither in basal nor osteogenic medium.

Figure 22. MC3T3-E1 differentiation study by collagen production (Sirius Red staining) on cells treated with 100 μg/ml of BB-derived materials and HA after 2 weeks culture.

Extracellular matrix mineralisation is also one of the major aspects of bone formation. Minerals formed *in vitro* were found to consist of calcium and phosphorus deposited on well-bonded collagen fibrils, and some of the crystals matured into hydroxyapatite crystals [58]. Besides its effect on ALP activity and collagen synthesis, we determined whether BB-derived materials might affect the mineralisation of the matrix formed by MC3T3-E1 cells. These cells are known to deposit minerals in the collagenous matrix in the presence of β-glycerol phosphate [59].

Extracellular matrix calcium deposits for mineralised nodule formation were stained with Alizarin red S dye which combines with calcium ions. After culturing MC3T3-E1 cells in the presence of BBM derived materials at 100 µg/mL for 15 days, the cells were then washed thrice with PBS and subsequently fixed in 75 % ethanol for 1 h. These cell cultures were then stained with 40 mM Alizarin Red S in distilled water (pH 4.2) for 10 min at room temperature. The cell monolayers were then washed with distilled water until no more colour appeared. The stain was dissolved in 10 % cetylpyridinium chloride in 10 mM sodium phosphate (pH 7.0) and the absorbance values at 620 nm were measured. The extracellular matrix mineralisation deter‐mined by Alizarin Red S staining is shown in Figure 23. In all of the tested conditions cells grown in osteogenic medium for 15 days displayed slightly higher calcium content, an indicator of mineralisation nodule formation. Treatment with BB-derived materials at a concentration of 100 µg/mL for 15 days did not significantly affect the mineralisation rates compared with those of control cells grown on polystyrene plates (Figure 23a). For these determinations HA (a material which contains Ca/P-apatite) could not be used as a control due to the high background produced by the material itself. These results indicated normal mineralisation induced by MC3T3-E1 cells in long-term cultures was not affected by the BB-derived materials.
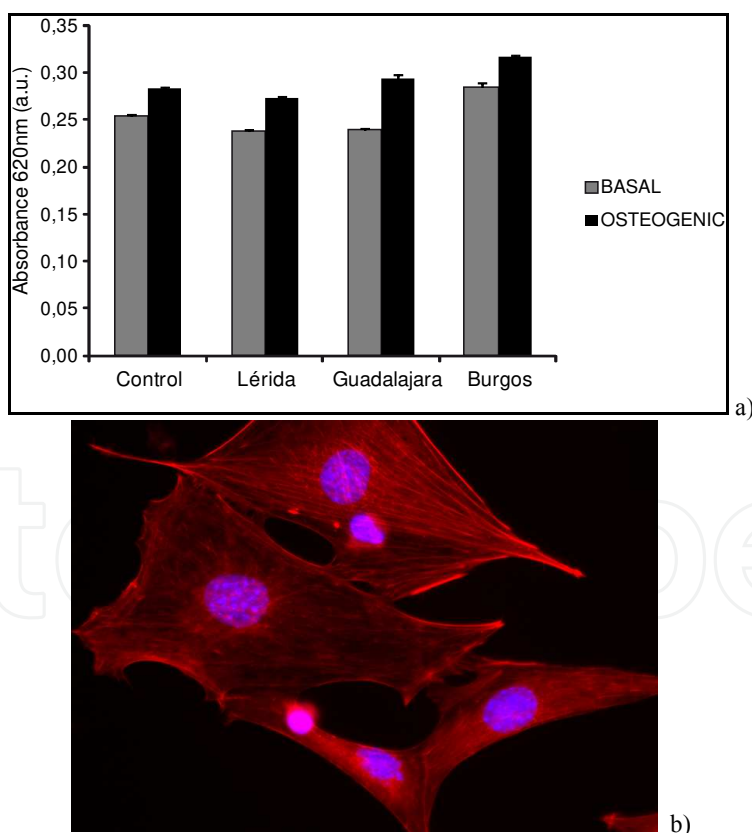
Figure 23. a) MC3T3-E1 differentiation study by extracellular matrix mineralisation (Alizarin Red S staining) on cells treated with 100 µg/ml of BBM derived materials after 2 weeks in culture. b) Osteoblasts (MC3T3-E1cells) growing in the presence of BBM derived materials. Cells were stained with phalloidine (red) and the nuclei were counterstained with ToPro-3 (blue).

Overall, in the presence of BB derived materials the osteoblast functions displayed normal cell differentiation profiles with respect to alkaline phosphatase activity, collagen secretion and extracellular matrix mineralisation. Furthermore, these parameters were maintained when compared to control cells grown on plastic plates and also with those obtained by culturing MC3T3-E1 cells in the presence of the same amounts of HA. The use of these BB-derived materials as coatings of metallic and ceramic bioimplants for odontoestomatologic treatments, or to form part of 3D scaffolds with pore sizes designed with the desired characteristics for bone replacement, is currently under study. Together the results suggest that the developed materials may potentially be used to prepare scaffolds for bone tissue engineering applications.

5.2. Controlled desorption of bioactive substances

The biological activity of a substance depends mainly on the nature of its interaction with the tissue or organ; it must reach the target in an amount that is adequate to produce the desired effect, which means that it should be liberated in the particular place at a controlled rate. The same amount of active ingredient can have different effects when it is formulated as oral solution or in capsules or pills, due to the different rates of adsorption of the active agents in the digestive track. These requirements mean that preparing drugs from pure substances is a multidisciplinary and extensive field that requires multidisciplinary expertise in pharmaceutical sciences, engineering, material sciences, physical chemistry, polymer science, solution chemistry and biochemistry, amongst others.

The work presented here is based on the use of beer and rice production residues to prepare materials with special characteristics towards controlled desorption of bioactive substances, using the anticarnogenic drug 5-Fluorouracil as the model molecule (Figure 24).
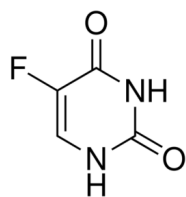

Figure 24. 5-Fluorouracil, anticarcinogen

The drug 5-fluorouracil (5-FU) is a pyrimidine analogue, used in the treatment of cancer, as it is an irreversible inhibitor of thymidylate synthase; interrupting the action of this enzyme blocks synthesis of the pyrimidine thymidine, nucleoside required for DNA replication [60]. 5-FU belongs to the World Health Organization's List of Essential Medicines, being part of the family of drugs called antimetabolites. It has been used amongst others in the treatment of breast, stomach, pancreatic and skin cancers. Its main disadvantage is that the same dose of 5-FU may have therapeutic response with low toxicity in some patients, while even life-threatening toxicity in others [61]. Thus, its use in a controlled manner is of great interest to avoid these problems. Parenteral administration causes a rapid elimination of 5-FU with an apparent terminal half-life of approximately 8-20 min. Choosing a proper controlled release

system can improve its anticancer activity and also decrease the adverse side effects. 5-FU is a neutral weak acid [62, 63] whose tautomers structures are shown in Figure 25.
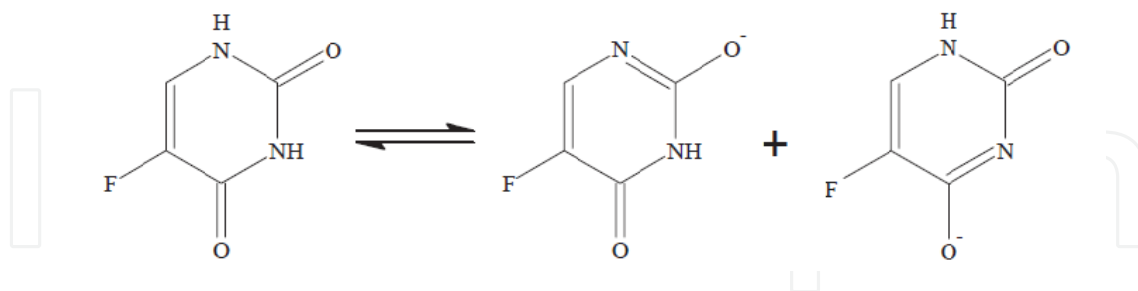

Figure 25. 5-FU tautomers

The design of materials to be used in desorption of bioactive substances is based on a thorough study of the conditions necessary to achieve a texture and structure capable to induce desorption in a controlled manner. The residues were first treated thermally to avoid putrefaction, as indicated above and then, according to TG-DTA analyses three different temperatures were chosen, *i.e.* 700, 850 and 1000°C, after previous studies by infrared spectroscopy (FTIR), textural analysis, X-ray diffraction and acetic acid decomposition on basic sites by TG-MS, and textural analyses by N_2 adsorption/desorption and mercury intrusion porosimetry. In this way the residue derived materials have different structure and surface characteristics, with higher crystallinities and lower surface areas, porosities and basic sites on their surfaces, on increasing the treatment temperature.

The biocompatibility of these bioecomaterials BBM47, BBM48 or BBM410 was studied after crushing and sieving, and homogeneized to a controlled particle size to favour reproducible results, according to previous studies. In order to assess the bioecomaterials biocompatibility a human glioblastoma cell line (1321N1) was used (Figure 26).
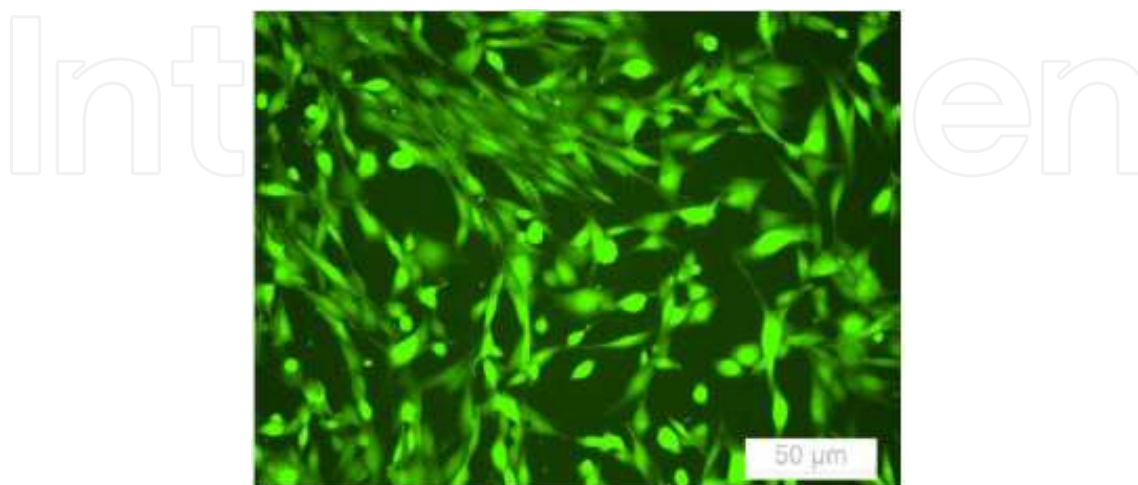
Figure 26. Images of 1321N1 cells stained with AM-calcein showing live cells.

The viability of 1321N1 cells growing in the presence of the materials was determined at 1, 3 and 7 days.The quantification of cell viability on the different materials (Figure 27) indicates that all the materials were biocompatible, with cell viabilities similar or even better than the plastic control up to 7 days.
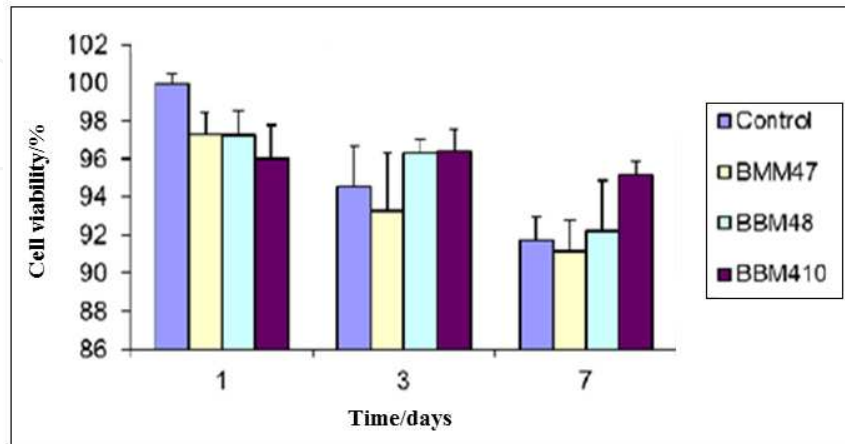
Figure 27. Cell viability (%) determined by MTT assay showing cells growing on biomaterials after 1, 3 and 7 days.

The preparation of the bioecomaterials to be used in controlled desorption was undertaken by studying different important parameters in their structuration, such as pelletising conditions, use of porogens, *etc.*. The particle size was controlled by sieving, and the conditions of pelletising (1 cm diameter) studied by changing the amount of material, pressure and time, being optimised at 5 tons pressure for 2 min. The material used was BBM47, since this had a higher surface area and porosity leading to a greater capacity for 5-FU absorption.

After the pellets were prepared, they were sintered, once again after the corresponding study of the temperature and time of sintering, since they are parameters of utmost importance. Experimental results indicated that the optimum temperature of sintering was 700 °C for 4 h. Lower temperatures or times did not produce pellets with enough cohesion and higher temperautres or times produced materials with lower surface areas and pore volumes.

To determine the 5-FU concentration needed to eliminate 1321N1 cells after 2 days in cultures, the MTT assay was used, as described above. The 1321N1 cells were cultured (20000 cells/well in 24-well plates) at 37 °C in 5 % CO_2 with 95 % humidity atmosphere for 24 h to favour their adhesion to the plates. Afterwards different concentrations of 5-FU were added to the medium and 2 days later the MTT assay was carried out.

From the results shown in Figure 28, it can be observed that a 5-FU concentration of 10 μg/mL was enough to eliminate all 1321N1 cells present in the culture. However, a concentration of 20 μg/mL was chosen, since it was possible that not all the adsorbed 5-FU would be liberated. Consequently, 200 μL of a solution 5-FU (20μg/mL) were added to each pellet, left to dry at room temperature for 24 h, protected from light, 5-FU is light sensitive. Finally the pellets were left in contact with human glioblastoma cells 1321N1, growing in DMEM (Gibco) supple-
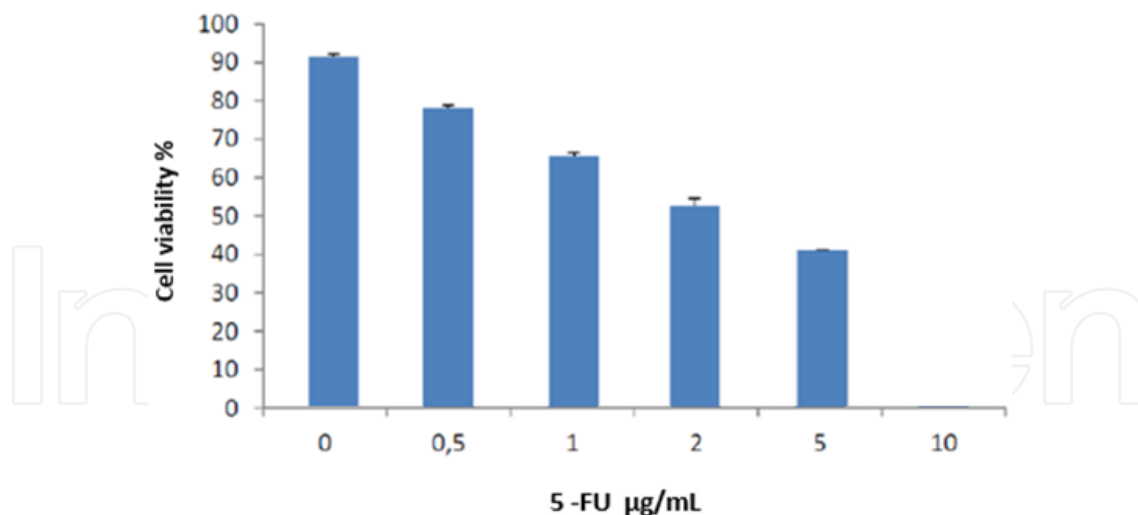
Figure 28. Cell viability after 2 days of treatment with different amounts of 5-FU (µg/mL).

mented with 10 % of bovine phoetal serum and 1 % peniciline/estreptomicine and the cell viability studied with fluorescent probes, as indicated above, following the decrease in cell viability as the 5-FU was desorbed from the pellets. The analyses of the desorption kinetics was carried out by comparison with the data obtained using a mesoporous silica prepared in our research group from rice husk (MR). This mesoporous material contains more than 97% silica, which is considered as ideal for desorption of pharmaceutical compounds [64].
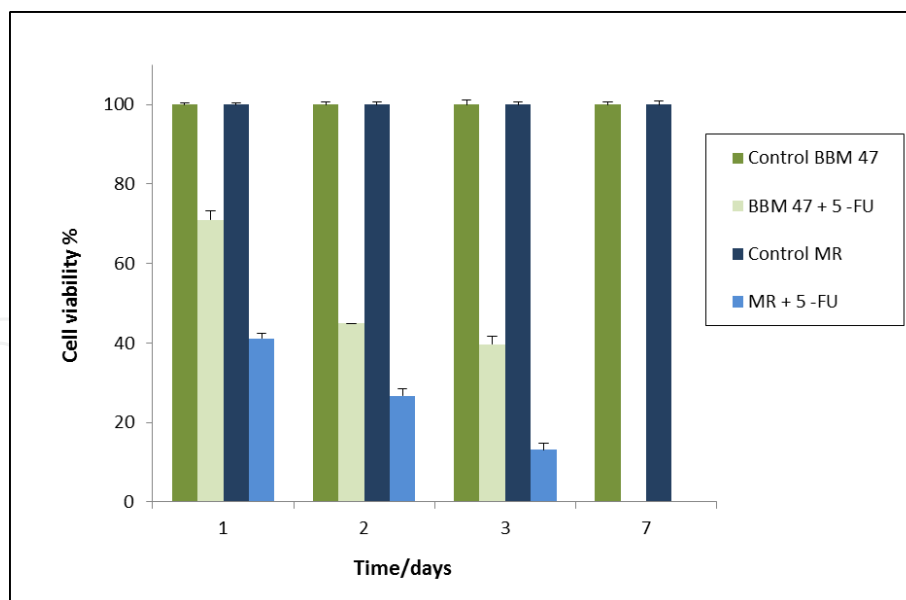
Figure 29. Viability of 1321N1 cells after 1, 2, 3 or 7 days in contact with BBM47 bioecomaterial or MR with 5-FU adsorbed.

According to these results, it can be said that 1321N1 cells could be eliminated with both materials, although BBM47 eliminates cancerous cells in a more controlled manner than MR. The characterisation of these materials indicates that MR was an amorphous mesopo-

rous silica with a surface area of 98 m^{2}g^{-1} and BBM was crystalline with silica in the form of cristobalite and calcium and magnesium phosphate of 4 m^{2}g^{-1}, also the basicity of BBM was much higher than that of MR, given its composition rich in alkaline earth cations (Figures 13 and 18), versus MR having more than 97% silica. The importance of the basic properties of the materials for the controlled release of 5-FU was to be expected, since given the acidity of 5-FU it would adsorb on basic sites. This explains why even though BBM47 had a much lower surface area than MR, its much higher basicity leads to a greater interaction with 5-FU, facilitating its controlled desorption, after careful design of its textural and structural characteristics [62, 65-67].

6. Conclusions

Residues from the beer, rice and sunflower oil production industries were used to prepare materials capable of cleaning wastewaters, support enzymes, act as catalysts or as scaffolds for tissue engineering or controlled desorption of bioactive substances. The use of these waste materials gives them an added value as a sustainable, environmentally friendly and economic supply of nanostructured materials, *i.e.* BBM derived materials obtained were as cytocompatible and osteogenic as HA powder, commonly used in bone and teeth replacement therapies, being non-cytotoxic and supporting cell growth and differentiation and of controlled desorption of anticarcinogen 5-Fluorouracil. Sunflower oil production residues can be used as raw materials to transform glycerol from biodiesel production of the same company towards fuel additives. Rice husk derived materials can be used to support enzymes in an inexpensive and environmentally sound way. Furthermore, the design of materials are based on preparation methods kept as simple and inexpensive as possible, with low energy consumption and easily adoptable procedures, by careful design of parameters and use of characterisation techniques used in materials engineering.

Acknowledgements

Author details

A.M. Martínez Serrano[1,2,3], M. Ramos[1], M. Yates[2], M.A. Martin-Luengo[3*], F. Plou[2],
J.L. Lacomba[4], G. Reilly[5], C. Vervaet[6], P. Muñoz[7], G. Garcia[8], J.L. Tarterra[9], B. Fite[9],
A. Urtzainki[10], M.C. Vidal[11], E. Sáez Rojo[3], L. Vega Argomaniz[2], A. Civantos[4] and V. Zurdo[3]

*Address all correspondence to: mluengo@icmm.csic.es

1 Polytechnic University of Madrid, Spain

2 Institute of Catalysis and Petroleochemistry, CSIC, Spain

3 Institute of Materials Science of Madrid, CSIC, Spain

4 Institute of Biofunctional Studies, Complutense University of Madrid, Spain

5 INSIGNEO Institute for in silico Medicine, Sheffield, UK

6 Laboratory of Pharmaceutical Technology, University of Ghent, Ghent, Belgium

7 Destilerias Muñoz Galvez S.A., Murcia, Spain

8 Acesur-Tarancon, Carretera Madrid-Valencia, Cuenca, Spain

9 Mahou-San Miguel S.A. Lleida, Spain

10 Createch Medical S. L., Pol. Kurutz Gain, Mendaro (Guipúzcoa), Spain

11 Maicerías Españolas, S.A. (DACSA), Spain

References

[1] 11th International Conference on Renewable Resources & Biorefineries 2015: Conference Proceedings, 3-5 June, 2015, York, United Kingdom.

[2] WasteEng 2014 - 5th International Conference on Engineering for Waste and Biomass Valorisation. August 25-28, 2014. Rio de Janeiro, Brazil.

[3] Braungart M, McDonough W. Editors. Cradle to Cradle: Remaking the Way We Make Things: North Point Press; 2002. ISBN-10: 0865475873

[4] Mirabella N, Castellani V, Serenella S. Current options for the valorization of food manufacturing waste: a review. Journal of Cleaner Production 2014; 65: 28-41.

[5] Ranade VV, Bhandary VM. Editors. Industrial Wastewater Treatment, Recycling and Reuse. Elsevier; 2014. ISBN: 978-0-08-099968-5

[6] Distilleries Muñoz Galvez (DMG). http://dmg.es/ (accessed 24 September 2014).

[7] Project CDTI IDI-20091139 (2010-2011) "Systems for recovery of aquoeous effluents with contaminants valorization and reduction of wastes. Total oxidation of contaminants in effluents through the use of Ecomaterials".

[8] Yates M, Martín-Luengo MA, Vega Argomaniz L, Nogales Velasco S. Design of activated carbon–clay composites for effluent decontamination. Microporous and Mesoporous Materials 2012; 154: 87-92.

[9] Yates M, Blanco J, Martín-Luengo MA, Martin MP. The dynamic adsorption behaviour of volatile organic compounds on activated carbon honeycomb monoliths. Studies in Surface Science and Catalysis 2002; 144: 569-576.

[10] Mahou San Miguel, Spain. http;//mahou-sanmiguel.com. (accessed 24 September 2014).

[11] Yates M, Martín-Luengo MA, Casal Piga B. Patent "Preparation of biocompatible materials from beer production residues and their uses". P200803331.

[12] Maicerías Españolas, S.A. DACSA, Spain. http://dacsa.com. (accessed 24 September 2014).

[13] Martín-Luengo MA, Yates M, Plou F, Lozano R, Saez E, Martínez Serrano AM, Vega L, Medina L, Zurdo V, Ramos M, Valero F, Benaiges MD. Patent "Procedure for production of an immobilized enzyme on a support derived from agroindustrial residues". P201330114.

[14] Martin-Luengo MA, Yates M, Diaz M. Renewable Fine Chemicals from rice and citric subproducts. Ecomaterials. Applied Catalysis B: Environmntal 2011; 106: 488-493.

[15] Visa M, Chelaru AM. Hydrothermally modified fly ash for heavy metals and dyes removal in advanced wastewater treatment. Renewable Energy Systems and Recycling. Applied Surface Science 2014; 303: 14-22.

[16] Yates M, Blanco J, Martin-Luengo MA, Martin MP. Vapour adsorption capacity of controlled porosity honeycomb monoliths. Microporous and Mesoporous Materials 2003; 65(2-3): 219-231.

[17] Martín-Luengo MA, Yates M, Martínez Domingo MJ, Casal B, Iglesias M, Esteban M, Ruiz-Hitzky E. Synthesis of *p*-cymene from limonene, a renewable feedstock. Applied Catalysis B: Environmental 2008; 81: 218-224.

[18] ISO 6060:1989. Water quality Determination of the chemical oxygen demand. http://iso.org/iso/catalogue_detail.htm?csnumber=12260

[19] Ali I, Asim M, Khan TA. Low cost adsorbents for the removal of organic pollutants from wastewater. Review. Journal of Environmental Management 2012; 113: 170-183.

[20] Souza J, Souza PMTG, de Souza PP, Sangiorge DL, Pasa VMD, Oliveira LCA. Production of compounds to be used as fuel additive: Glycerol conversion using Nb-doped MgAl mixed oxide. Catalysis Today 2013; 213: 65-72.

[21] Martin A, Richter M. Oligomerization of glycerol - a critical review. European Journal of Lipid Science and Technology 2011; 113: 100–117.

[22] Project CDTI IDI-20111090 (IDI-20121298) (2012-2014) "Valorization of glycerine subproduct of biodiesel production. Comparison of conventional catalysts and Ecomaterials from own agriresidues".

[23] Behr A, Eilting J, Irawadi K, Leschinski J, Lindner F. Improved utilisation of renewable resources: New important derivatives of glycerol. Green Chemistry 2008; 10: 13-30.

[24] Bagheri S, Julkapli NM, Yehye WA. Catalytic conversion of biodiesel derived raw glycerol to value added products. Review Article. Renewable and Sustainable Energy Reviews 2015; 41: 113-127.

[25] Barrault J, Clacens JM, Pouilloux Y. Selective Oligomerization of Glycerol over Mesoporous Catalysts. Topics in Catalysis 2004; 27: 137–142.

[26] Ruppert AM, Meeldijk JD, Kuipers BWM, Erné BH, Weckhuysen BM. Glycerol Etherification over Highly Active CaO-Based Materials: New Mechanistic Aspects and Related Colloidal Particle Formation. Chemistry- A European Journal 2008; 14(7): 2016-2024.

[27] Barrault J, Jerome F. Design of new solid catalysts for the selective conversion of glicerol. European Journal of Lipid Science and Technology 2008; 110(9): 825-830.

[28] Cassel S, Debaig C, Benvegnu T, Chaimbault P, Lafosse M, Plusquellec D, Rollin P. Original Synthesis of Linear, Branched and Cyclic Oligoglycerol Standards. European Journal of Organic Chemistry 2001; 5: 875–896.

[29] Perozo Rondon E. Basicity in catalysis. A contribution to Green Chemistry. PhD thesis. UNED Madrid; 2008.

[30] Medeiros MA, Araujo MH, Augusti R, Oliveira LCA, LagoRM. Acid-catalyzed oligomerization of glycerol investigated by electrospray ionization mass spectrometry. Journal of the Brazilian Chemical Society 2009; 20: 1667-1673.

[31] Oliveira LCA, Portilho MF, Silva AC, Taroco HA, Souza PP. Modified niobia as a bifunctional catalyst for simultaneous dehydration and oxidation of glycerol. Applied Catalysis B: Environmental 2012; 117–118: 29-35.

[32] Gholami Z, Abdullah AZ, Lee KT. Glycerol etherification to polyglycerols using a $Ca_1+xAl_1-xLa_xO_3$ composite catalyst in a solventless medium. Journal of the Taiwan Institute of Chemical Engineers 2013; 44: 117-122.

[33] Gil S, Marchena M, Sánchez-Silva L, Romero A, Sánchez P, Valverde JL. Effect of the operation conditions on the selective oxidation of glycerol with catalysts based on

Au supported on carbonaceous materials. Chemical Engineering Journal 2011; 178: 423-435.

[34] Sivaiah MV. Recent developments in acid and base-catalyzed etherification of glycerol to polyglycerols. Review. Catalysis Today 2012; 198: 305-313.

[35] Martín-Luengo MA, Yates M, Ramos M, Martínez AM, Sáez E, Martin Aranda RM, Sanz J, Gil L. Patent "Procedure to obtain multifunctional and renewable materials from sunflower oil production residues" P201130303.

[36] Calero-Rueda O, Barba V, Rodríguez E, Plou FJ, Martínez AT, Martínez MJ. Study of a sterol esterase secreted by Ophiostoma piceae: Sequence, model and biochemical properties. Biochimica et Biophysica Acta (BBA) - Proteins and Proteomics 2009; 194(7): 1099-1106.

[37] Barba V, Plou FJ, Calero-Rueda O, Martínez AT, Martínez MJ. Native and recombinant sterol esterases from Ophiostoma piceae: enzymes with high biotechnological potential. New Biotechnology 2009; 25: S136.

[38] Alcalde M, Ferrer M, Plou FJ, Ballesteros A. Environmental biocatalysis: from remediation with enzymes to novel green processesReview Article. Trends in Biotechnology 2006; 24(6): 281-7.

[39] Hu Q, Tan Z, Liu Y, Tao J, Cai Y, Zhang M, *et al.* Effect of crystallinity of calcium phosphate nanoparticles on adhesion, proliferation, and differentiation of bone marrow mesenchymal stem cells. Journal of Materials Chemistry 2007; 17: 4690-8.

[40] Polo-Corrales L, Latorre-Esteves M, Ramirez-Vick JE. Scaffold design for bone regeneration. Journal of Nanoscience and Nanotechnology 2014; 14: 15-56.

[41] Puppi D, Detta N, Piras AM, Chiellini F, Clarke DA, Reilly GC, *et al*. Development of Electrospun Three-arm Star Poly (ε-caprolactone) Meshes for Tissue Engineering Applications. Macromolecular Bioscience 2010; 10; 887-897.

[42] Hou Q, De Bank PA, Shakesheff KM. Injectable scaffolds for tissue regeneration. Journal of Materials Chemistry 2004; 14: 1915-1923.

[43] Bandyopadhyay A, Bernard S, Xue W, Bose S. Calcium Phosphate-Based Resorbable Ceramics: Influence of MgO, ZnO, and SiO_2 Dopants. Journal of the American Ceramic Society 2006; 89: 2675-2688.

[44] Pietak AM, Reid JW, Stott MJ, Sayer M. Silicon substitution in the calcium phosphate bioceramics.Biomaterials, 2007; 28: 4023-4032.

[45] Kim EJ, Bu SY, Sung MK, Choi MK. Effects of Silicon on Osteoblast Activity and Bone Mineralization of MC3T3-E1 Cells. Biological Trace Elements Research 2013; 152: 105-112.

[46] Zhao SF, Jiang QH, Peel S, Wang XX, He FM. Effects of magnesium-substituted nanohydroxyapatite coating on implant osseointegration. Clinical Oral Implants Research 2011; 24: 34-41.

[47] Wei J, Jia J, Wu F, Wei S, Zhou H, Zhang H, *et al*. Hierarchically microporous/macroporous scaffold of magnesium-calcium phosphate for bone tissue regeneration. Biomaterials 2010; 31: 1260-9.

[48] Martin-Luengo MA, Yates M, Ramos M, Saez Rojo E, Martinez Serrano AM, Gonzalez Gil, L. Biomaterials from beer manufacture waste for bone growth scaffolds. Green Chemistry Letters and Reviews 2011; 4: 229-233.

[49] Martin-Luengo MA, Yates M, Ramos M, Plou F, Salgado JL, Lacomba JL, Reilly G, Vervaet C. Sustainable materials and biorefinery chemicals from agriwastes. In:.V. Abrol V., Sharma P. in Resource management for sustainable agriculture: Intech: 2012, p19-38. Available from http://www.intechopen.com/books/resource-management-for-sustainable-agriculture

[50] Saez Rojo E, Ramos M, Yates M, Martin-Luengo MA, Martínez Serrano MA, Civantos A, *et al*. Preparation, characterization and in vitro osteoblast growth of waste-derived biomaterials. Royal Society Advances 2014; 4: 12630-9. Project INNPACTO IPT-2011-1935-310000 (2011-2014).

[51] Wang D, Christensen K, Chawla K, Xiao GZ, Krebsbach PH, Franceschi RH. Isolation and Characterization of MC3T3-E1 Preosteoblast Subclones with Distinct In Vitro and In Vivo Differentiation/Mineralization Potential. Journal of Bone Mineral Research 1999; 14: 893-899.

[52] Quarles LD, Yohay DA, Lever LW, Caton R, Wenstrup RJ. Distinct proliferative and differentiated stages of murine MC3T3-E1 cells in culture: An *in vitro* model of osteoblast development. Journal of Bone and Mineral Research, 1992; 7: 683-692.

[53] Puleo D, Preston K, Shaffer J, Bizios R. Examination of osteoblastorthopaedic biomaterial interactions using molecular techniques. Biomaterials 1993; 14: 111-4.

[54] Valerio P, Pereira MM, Goes AM, Leite MF. The effect of ionic products from bioactive glass dissolution on osteoblast proliferation and collagen. Biomaterials 2004; 25: 2941-8.

[55] Koh YH, Bae CJ, Sun JJ, Jun IK, Kim HE. Macrochanneled poly (⊚-caprolactone)/ hydroxyapatite scaffold by combination of bi-axial machining and lamination. Journal of Materials Science: Materials in Medicine 2006; 17: 773-784.

[56] Budiraharjo R, Neoh KG, Kang ET. Hydroxyapatite-coated carboxymethyl chitosan scaffolds for promoting osteoblast and stem cell differentiation. Journal of Colloid and Interface Science 2012; 366: 224-232.

[57] Kannan S, Vieira SI, Olhero SM, Torres PM, Pina S, Silva OAC et al. Synthesis, mechanical and biological characterization of ionic doped carbonated hydroxyapatite/β-tricalcium phosphate mixtures. Acta Biomaterialia 2011; 7: 1835-1843.

[58] Fratzl-Zelman N, Fratzl P, Hörandner H, Grabner B, Varga F, Ellinger A, *et al.* Matrix mineralization in MC3T3-E1 cell cultures initiated by β-glycerophosphate pulse. Bone 1998; 23; 511-520.

[59] Sudo H, Kodama HA, Amagai Y, Yamamoto S, Kasai S. In vitro differentiation and calcification in a new clonal osteogenic cell line derived from newborn mouse calvaria. Journal of Cell Biology 1983; 96: 191-8.

[60] Longley DB, Harkin DP, Johnston PG. 5-fluorouracil: mechanisms of action and clinical strategies. Nature Reviews 2003; 3(5): 330–8.

[61] Brayfield, A, ed. (13 December 2013). "Fluorouracil". Martindale: The Complete Drug Reference. Pharmaceutical Press. "WHO Model List of EssentialMedicines". World Health Organization. October 2013.

[62] Wang Z, Wang E, Gao L, Xu L. Synthesis and properties of Mg2Al layered double hydroxides containing 5-fluorouracil. Journal of Solid State Chemistry 2005; 178: 736–741.

[63] Diasio RB, Harris BE. Clinical pharmacology of 5-fluorouracil. Clinical Pharmacokinetics 1989; 16: 215-37.

[64] Roik NV, Belyakova LA. Chemical design of pH-sensitive nanovalves on the outer surface of mesoporous silicas for controlled storage and release of aromatic amino acid. Journal of Solid State Chemistry 2014; 215: 284-291

[65] Santos MA Martins RP, Franke MM, Almeida MEV. Calcium phosphate granules for use as a 5-Fluorouracil delivery system Ceramics International 2009; 35:1587-1594.

[66] Datt A, Burns EA, Dhuna NA, Larsen SC. Loading and release of 5-fluorouracil from HY zeolites with varying SiO_2/Al_2O_3 ratios. Microporous and Mesoporous Materials 2013; 167: 182-187.

[67] Cosijns A, Vervaet C, Luyten J, Mullens S, Siepmann F, Van Hoorebeke L, Masschaele B, Cnudde V, Remon JP. Porous hydroxyapatite tablets as carriers for low-dosed drugs. European Journal of Pharmaceutics and Biopharmaceutics 2007; 67: 498-506.